Analysis of PI-Control for Atomic Force Microscopy in Contact Mode

Saverio Messineo, Michael R. P. Ragazzon, *Member, IEEE*, Fabio Busnelli, and Jan Tommy Gravdahl, *Senior Member, IEEE*

***Abstract*— This article investigates the properties, from a nonlinear control system standpoint, of atomic force microscope (AFM) systems, whenever operated in contact mode and controlled in the vertical direction by proportional-integral control law. By modeling the AFM as a system in which a piezo-electric actuator and a cantilever mutually interact in order to produce the sample topography, ensuing distortions affecting the quality of the yielded topography measurement are naturally cast and analyzed. The proposed investigation considers distortions due to the inception of hysteresis and vibrational dynamics within the piezo-actuator or provoked by system saturation. Both hysteresis and saturation are inherently nonlinear phenomena and are modeled as such. In spite of the inherently nonlinear nature of the AFM dynamics, investigations of the contact mode case from a nonlinear standpoint are lacking within the AFM literature. As the topography yielded by the AFM completely relies on its control algorithm, to the point that the measurement itself *corresponds* to the control action $v(t)$, it becomes of paramount importance to understand how $v(t)$ relates to the actual topography, and how such a relationship is affected by the aforementioned distortions. This article hence intends to contribute to the AFM literature, by providing a study in which the very meaning of the image measurement yielded by the AFM is investigated, in the light of distortions due to nonlinear phenomena. The AFM is considered to be operated in contact mode with a PI algorithm. Furthermore, as a byproduct of the derived nonlinear stability analysis, a novel, model-based algorithm for tuning the PI control gains is provided. Finally, experimental results are presented and analyzed in view of the derived theory.**

***Index Terms*— Atomic force microscope (AFM) control, nonlinear control, normal form, singular-perturbation form, small-gain arguments, Tikhonov's theorem, zero dynamics.**

I. Introduction

THE atomic force microscope (AFM) is a powerful device capable of yielding sample-surface measurements with nanometer resolution [1], [2].

Manuscript received March 29, 2021; revised August 22, 2021; accepted October 4, 2021. Manuscript received in final form October 17, 2021. Recommended by Associate Editor A. Serrani. *(Corresponding author: Saverio Messineo.)*

Saverio Messineo, Michael R. P. Ragazzon, and Jan Tommy Gravdahl are with the Department of Engineering Cybernetics, Norwegian University of Science and Technology (NTNU), 7034 Trondheim, Norway (e-mail: saverio.messineo@ieee.org; michael.remo.ragazzon@ntnu.no; jan.tommy.gravdahl@ntnu.no).

Fabio Busnelli is with the Dipartimento di Elettronica, Informazione e Bioingegneria, Politecnico di Milano, 20133 Milan, Italy (e-mail: fabusnelli@gmail.com).

Color versions of one or more figures in this article are available at https://doi.org/10.1109/TCST.2021.3121321.

Digital Object Identifier 10.1109/TCST.2021.3121321

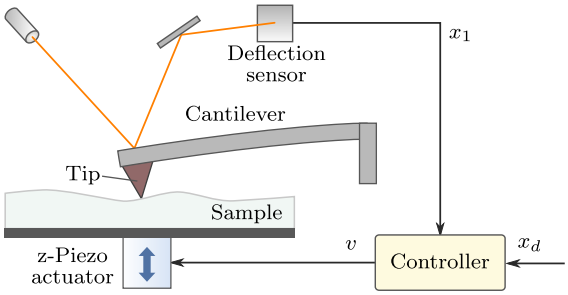

Fig. 1. Vertical control loop of an AFM operating in contact mode.

A typical AFM setup, see Fig. 1, is composed of a sharp tip mounted on one extremity of a cantilever, which, in turn, is attached to a piezoelectric actuator, referred to as the z-piezo. By receiving and processing the reflection of a laser beam, a position-sensitive photodetector (PSPD) is employed to detect and yield the deflection of the cantilever which is used for feedback purposes. The cantilever deflection is the result of the interatomic force interplay between the sample and the cantilever in the form of attracting van der Waals forces or repulsive Pauli forces, which are inherently nonlinear phenomena [2, p. 910].

AFMs are usually operated in one of two distinct modes: contact mode (static mode) or oscillating mode (dynamic mode) [1, ch. 3]. In this article, the AFM is investigated while operating in contact mode. In this mode, the information about the sample topography is acquired while the cantilever's tip is in contact with the sample. As the sample is scanned, interatomic force interactions produce a mismatch between the actual cantilever's deflection and a reference one. Such mismatch is used within a feedback loop in order to regulate the cantilever's deflection toward a reference constant value. The topography of the sample is then provided in the form of the time history of the control effort itself employed to pursue the regulation task.

The main task of this article is to analyze this very measurement mechanism, that is, to investigate the extent to which the time history of the control effort is capable of providing a reliable representation of the actual sample topography. The analysis is pursued for AFMs, whenever operated in contact mode and controlled in the vertical direction by a PI control law. The PI algorithm, usually embedded in commercial AFMs, is one of the most common imaging configurations.

By modeling the AFM as a *nonlinear* system in which a piezo-electric actuator and a cantilever mutually interact to

produce the sample-topography, ensuing distortions hampering the quality of the yielded topography-measurement, are naturally cast and analyzed. This investigation considers distortions due to hysteresis and vibrational dynamics induced by the piezo-actuator, as well system saturation. Both hysteresis and saturation are inherently nonlinear phenomena and are modeled as such. Indeed, in spite of the inherently nonlinear nature of the AFM dynamics, investigations of the contact mode case from a nonlinear standpoint have remained so far elusive. In particular, to the authors' knowledge, no study has investigated the effects provoked by such distortions on the very meaning of the yielded measurement-output displayed on the screen: what is indeed the meaning of the measurement displayed on the screen? This article hence intends to contribute to the AFM literature by filling these gaps.

By employing nonlinear arguments originating within the framework of the small-gain theorem [3, p. 36], and by exploiting system representations such as the normal form [4, ch. 4] and the singular-perturbation form [5, ch. 11], operational regions within which the saturation limits are not exceeded, are characterized in terms of invariant Lyapunov level-sets. By then exploiting the derived stability results, and aided by an application of Tikhonov's theorem for infinite-time intervals [5, p. 439], the relationship between the time history of the control effort $v(t)$ and the cantilever-sample interaction force is provided, thereby highlighting the alterations caused by the aforementioned system's distortions on the yielded topography $v(t)$. In so doing, by dissecting and analyzing the actual nature (i.e., its *meaning*) of the yielded measurement $v(t)$, this work exposes the inherent limitations attached to representing the actual image-topography by using $v(t)$. This result, and the concurrent nonlinear analysis carried out to produce it, are both novelties and considered by the authors as original contributions.

Furthermore, as a byproduct of the derived stability analysis, a novel, model-based algorithm for tuning the PI control gains is proposed, which provides a complementary contribution to the article. Finally, experimental results are presented and analyzed in light of the derived results.

The article is organized as follows: in Section II, a mathematical model of the AFM system is presented, along with a formal definition of the problem under consideration. Section III focuses on the PI-controlled cantilever dynamics, Section IV revolves around the analysis of the piezo-actuator vibrational dynamics, whereas in Section V the properties of the entire closed-loop system are investigated. By then building on the derived results, Section VI —which is central within this work—analyzes the very "meaning" of the yielded topography measurement in the light of the alterations on the measurement output produced by the abovementioned system's distortions. Finally, in Section VII, experimental results are provided and discussed, followed by concluding remarks in Section VIII.

II. AFM-Modeling and Problem Definition

In this section, a formal description of the dynamics governing the behavior of the AFM system, when operated in contact mode and controlled by a PI control law, will be provided.

To this end, the AFM system is modeled as an architecture whereby a piezo-electric actuator and a cantilever interact in real-time in order to form and yield the sample topography. Within this architectural framework, the effect due to a potential system saturation on the commanded control signal $v(t)$ is described by the following input–output relationship:

$$\bar{v}(t) = \sigma(v(t)) \tag{1}$$

where the operator $\sigma(\cdot)$ models the alteration on the desired control input caused by a possible system saturation. The operator $\sigma(s)$ is modeled as a uniformly bounded differentiable real function (with a uniformly bounded derivative) of a real argument $\sigma(s)$, which equals the identity operator $\mathrm{id}(\cdot)$ for $|s| \leq \Delta$ (where $\Delta > 0$ represents the system's saturation limit), and deteriorates nonlinearly (possibly "fast," but yet in a differentiable fashion) for $|s| > \Delta$, and which converges to finite values for $s \to -\infty$ and $s \to \infty$. An example of such function is given by

$$\sigma(s) = \begin{cases} \Delta + \beta \ \mathrm{arctg}\left(\dfrac{1}{\beta}(s-\Delta)\right), & \text{for } s > \Delta \\ s, & \text{for } |s| \leq \Delta \\ -\Delta + \beta \ \mathrm{arctg}\left(\dfrac{1}{\beta}(s+\Delta)\right), & \text{for } s < -\Delta \end{cases}$$

where $\beta > 0$ is a parameter to be chosen according to the modeling needs.

Remark 2.1: From the physics of the piezoelectric actuators, it is known [1, p. 15] that there exists a maximum voltage the piezoelectric ceramics are capable to withstand before undergoing depolarization. With this being the case, while operating the AFM for carrying out experiments, it is fundamental to explicitly enforce a bound—or a "saturation"—onto the allowable range of voltages reaching the piezoelectric actuator. Such bound may be enforced by limiting on purpose the allowable output voltages produced by the amplifier connected to the input of the piezoelectric actuator, or by setting those limits directly within the AFM control software, or, if the experiments are carried out by using a real-time platform like dSpace, by placing an explicit saturation operator limiting the output of the designed control action, at Simulink level. Nonetheless, a form of system saturation must be necessarily imposed to protect the piezoelectric actuator.

The voltage-control signal, from the output of (1) then reaches the input of the piezoelectric actuator, which in turn exerts a distortion on $\bar{v}(t)$, whose effect is modeled here, as in [6], by means of a hysteresis operator followed by vibrational dynamics. The exerted distortion due to hysteresis is modeled as the action of an operator $q(\cdot)$ on $\bar{v}(t)$ whose effect is described by the following ordinary differential equation:

$$\dot{q}(t) = \bar{\alpha}\left|\dot{\bar{v}}(t)\right|(\bar{a}\bar{v}(t) - q(t)) + \bar{b}\dot{\bar{v}}(t) \tag{2}$$

that is, by the Duhem model (see [7]), where $\bar{\alpha} > 0$ and $\bar{a} > 0$ in (2), and whose solution, by following [8], [9], can be expressed in explicit form as:

$$q(t) = \bar{\alpha}\sigma(v(t)) + h(\bar{v}(t)) \tag{3}$$

where $h(\cdot)$ is a uniformly bounded operator. By then setting $u(t) = q(t)$, inspired by the work in [10], the piezo-electric

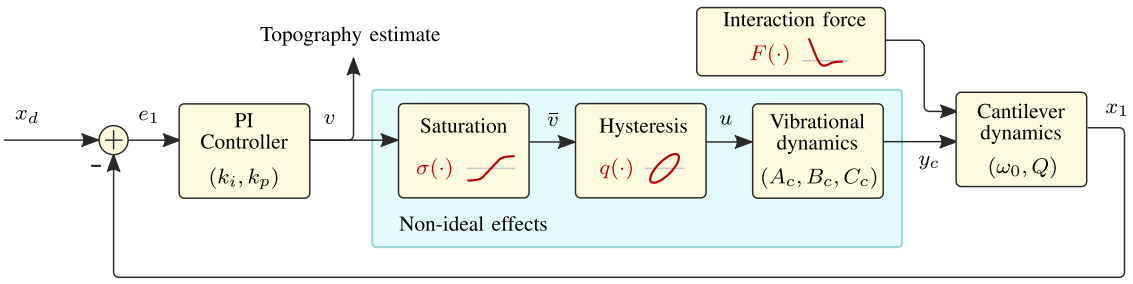

Fig. 2. Block diagram of the vertical AFM model and feedback loop. Brown symbols designate nonlinear effects. Linear systems are shown together with the symbols used to represent their parameterization.

actuator's vibrational dynamics is modeled by a singularly perturbed linear system of the form

$$\begin{aligned} \epsilon \dot{x}_c &= A_c x_c + B_c u(t) \\ y_c &= C_c x_c \end{aligned} \tag{4}$$

with A_c Hurwitz and $\epsilon > 0$. Following [2, pp. 916–917], the AFM cantilever is modeled as a lumped-parameters dynamical system of the form

$$\begin{aligned} \dot{x}_1 &= x_2 \\ \dot{x}_2 &= -\omega_0^2(x_1 - y_c) - \frac{\omega_0}{Q}(x_2 - \dot{y}_c) + \frac{1}{m}F(\cdot) \end{aligned} \tag{5}$$

where x_1 represents the cantilever position, ω_0 denotes the cantilever resonance frequency, $Q = (m\omega_0/\bar{d})$ the quality factor, $\bar{d}$ the damping coefficient, m the mass, whereas $F(\cdot)$ describes the cantilever-sample interaction force. A block diagram summarizing the AFM architecture proposed in this article—along with the feedback loop—is displayed in Fig. 2.

The AFM-control task entails steering the cantilever position to a constant, desired value, henceforth denoted by x_d. In conformity with this task, a preliminary change of coordinates is carried out by defining a set of regulation-error coordinates as $e_1 = x_1 - x_d$, $e_2 = x_2$, and by then rewriting the cantilever dynamics (5) in the newly defined coordinates, as

$$\begin{aligned} \dot{e}_1 &= e_2 \\ \dot{e}_2 &= -k(e_1 - y_c) - d(e_2 - \dot{y}_c) - kx_d + \frac{1}{m}F(\cdot) \end{aligned} \tag{6}$$

where $k = \omega_0^2$ and $d = (\omega_0/Q)$ have been defined with the purpose of easing the notation.

Since the right-hand side of (6) displays the derivative $\dot{y}_c$, it is convenient to perform an additional change of coordinates in order to remove it. The new coordinate framework $(e_1, z)^T$ is thus defined by keeping e_1 unaltered, and by setting

$$e_2 = \alpha_1 z + \alpha_2 e_1 + \alpha_3 y_c \tag{7}$$

where α_i $i = 1, \ldots, 3$ are constants to be determined. By virtue of (7), the cantilever dynamics in (6) can be given the following formal expression:

$$\begin{aligned} \dot{z} &= \frac{1}{\alpha_1}(\dot{e}_2 - \alpha_2 \dot{e}_1 - \alpha_3 \dot{y}_c) \\ \dot{e}_1 &= \alpha_1 z + \alpha_2 e_1 + \alpha_3 y_c \end{aligned} \tag{8}$$

from which, by using (6), it follows that:

$$\begin{aligned} \dot{z} = \frac{1}{\alpha_1}(&-ke_1 + ky_c - d(\alpha_1 z + \alpha_2 e_1 + \alpha_3 y_c) \\ &+ d\dot{y}_c - kx_d + \frac{1}{m}F(\cdot) - \alpha_2\alpha_1 z - \alpha_2^2 e_1 \\ &- \alpha_2\alpha_3 y_c - \alpha_3 \dot{y}_c) \\ \dot{e}_1 = \alpha_1 z + \alpha_2 e_1 + \alpha_3 y_c. \end{aligned} \tag{9}$$

The constants α_i, $i = 1, \ldots, 3$ are now to be selected with the aim of removing both y_c and $\dot{y}_c$ from the right-hand side of the first equation in (9). This is readily accomplished by choosing α_i, $i = 1, \ldots, 3$, such that the following holds:

$$\begin{aligned} d\dot{y}_c - \alpha_3 \dot{y}_c &= 0 \\ ky_c - d\alpha_3 y_c - \alpha_2\alpha_3 y_c &= 0. \end{aligned} \tag{10}$$

Equation (10) are fulfilled if and only if $\alpha_2 = (k - d^2/d)$ and $\alpha_3 = d$; moreover, for the change of coordinates in (7) to be well defined, it is necessary that α_1 be different from zero. Hence, the following conditions must be enforced in (9):

$$\begin{aligned} \alpha_1 &\neq 0 \\ \alpha_2 &= \frac{k - d^2}{d} \\ \alpha_3 &= d. \end{aligned} \tag{11}$$

By choosing for convenience $\alpha_1 > 0$, by defining $a = (k/d) > 0$, $b = -(1/\alpha_1)(k + d((k - d^2/d)) + ((k - d^2/d))^2)$ and $d_1(\cdot) = (1/\alpha_1)(-kx_d + (1/m)F(\cdot))$, by virtue of the conditions in (11), after some algebra, system (9) can be rewritten in normal form as

$$\begin{aligned} \dot{z} &= -az + be_1 + d_1(\cdot) \\ \dot{e}_1 &= \alpha_1 z + \frac{k - d^2}{d}e_1 + dy_c \end{aligned} \tag{12}$$

with $a > 0$, and where the disturbance $d_1(\cdot)$ is uniformly bounded by construction, since the force $F(\cdot)$ is a uniformly bounded quantity (see [11]–[16]). By then choosing the following PI dynamical control law

$$\begin{aligned} \dot{e}_0 &= e_1 \\ v(t) &= -k_i e_0 - k_p e_1 \end{aligned} \tag{13}$$

with $k_i > 0$, $k_p > 0$, from (1)–(4), (12), (13), the closed-loop system to be analyzed can be given the following form:

$$\begin{aligned}\epsilon\dot{x}_c &= A_c x_c + B_c u(t)\\ \dot{z} &= -az + be_1 + d_1(\cdot)\\ \dot{e}_0 &= e_1\\ \dot{e}_1 &= \alpha_1 z + \frac{k-d^2}{d}e_1 + dC_c x_c\\ u(t) &= \bar{\alpha}\sigma(-k_i e_0 - k_p e_1) + h(\cdot)\end{aligned} \tag{14}$$

where (2) has not been explicitly included in (14) since $q(t)$ in (2) allows for an explicit representation from (3), and where, by construction, $u(t) = q(t)$ in (14).

By subsequently defining a backstepping-based change of coordinates [17] as

$$\tilde{e}_1 = e_1 + \alpha e_0 \tag{15}$$

system (14) can be written as

$$\begin{aligned}\epsilon\dot{x}_c &= A_c x_c + B_c u(t)\\ \dot{z} &= -az + b\tilde{e}_1 - b\alpha e_0 + d_1(\cdot)\\ \dot{e}_0 &= -\alpha e_0 + \tilde{e}_1\\ \dot{\tilde{e}}_1 &= \alpha_1 z + \frac{k-d^2}{d}\tilde{e}_1 - \alpha\frac{k-d^2}{d}e_0 + dC_c x_c\\ &\quad - \alpha^2 e_0 + \alpha\tilde{e}_1\\ u(t) &= \bar{\alpha}\sigma(-(k_i - \alpha k_p)e_0 - k_p\tilde{e}_1) + h(\cdot).\end{aligned} \tag{16}$$

Finally, the following well-defined (since A_c is Hurwitz) change of coordinates is pursued:

$$\tilde{x}_c = x_c + A_c^{-1}B_c u \tag{17}$$

by virtue of which, system (16) can be further rewritten as

$$\begin{aligned}\dot{\tilde{x}}_c &= \frac{1}{\epsilon}A_c\tilde{x}_c + A_c^{-1}B_c\dot{u}(t)\\ \dot{z} &= -az + b\tilde{e}_1 - b\alpha e_0 + d_1(\cdot)\\ \dot{e}_0 &= -\alpha e_0 + \tilde{e}_1\\ \dot{\tilde{e}}_1 &= \alpha_1 z + \frac{k-d^2}{d}\tilde{e}_1 - \alpha\frac{k-d^2}{d}e_0\\ &\quad - d\ C_c A_c^{-1}B_c u(t) + dC_c\tilde{x}_c - \alpha^2 e_0 + \alpha\tilde{e}_1\\ u(t) &= \bar{\alpha}\sigma(-(k_i - \alpha k_p)e_0 - k_p\tilde{e}_1) + h(\cdot)\end{aligned} \tag{18}$$

where, by using (2) and (18), the derivative of the control action $\dot{u}(t)$ in (18) is seen to satisfy

$$\dot{u} = \bar{\alpha}\left|\frac{\partial\sigma(\bar{e})}{\partial\bar{e}}f(\cdot)\right|(a - \bar{\alpha})\sigma(\cdot) + b\frac{\partial\sigma(\bar{e})}{\partial\bar{e}}f(\cdot) \tag{19}$$

with $\bar{e} = -(k_i - \alpha k_p)e_0 - k_p\tilde{e}_1$, and $f(\cdot)$ defined as

$$\begin{aligned}f(\cdot) &= -\left(k_p\frac{k-d^2}{d} + k_i - \alpha k_p\right)\tilde{e}_1\\ &\quad + \left(k_p\alpha\frac{k-d^2}{d} + k_i\alpha + \alpha^2 k_p\right)e_0\\ &\quad - k_p\alpha_1 z - k_p dC_c\tilde{x}_c + k_p dC_c A_c^{-1}B_c u(t).\end{aligned} \tag{20}$$

In the next three sections, the stability properties of the dynamical system (18)–(20) describing the PI-control scheme applied to the AFM are investigated. By exploiting the inherently modular structure within the dynamics in (18), the analysis is structured in three distinct but mutually intertwined units. In the first one (Section III), the properties of the PI-controlled cantilever dynamics are investigated in relation to the control gains k_p and k_i and to the saturation limit Δ, by regarding the state $\tilde{x}_c(t)$ as an exogenous disturbance. In an analogous fashion, by regarding the states $z(t)$, $e_0(t)$ and $\tilde{e}_1(t)$ as incoming disturbances, the stability properties of the actuators dynamics (in $\tilde{x}_c$ coordinates) are studied in relation to the time-scale separation existing between the latter and the forced, controlled cantilever dynamics. This is done by determining the conditions by which ϵ "dominates" $\dot{u}$ in the first equation within (18). Finally, the stability properties of the whole system are investigated in Section V, by exploiting the derivations of the previous two sections.

III. PI-Controlled Cantilever Dynamics

The aim of this section is to focus on the PI-controlled cantilever dynamics within (18), and to analyze its behavior in relation to the time-evolution of the interatomic force interaction, of the piezo-actuator vibrational dynamics (in $\tilde{x}_c$ coordinates) and the hysteresis perturbation, by regarding such quantities as exogenous disturbances.

In view of this task, by then considering the saturation limit Δ previously defined, the set of the states $e_0(t)$ and $\tilde{e}_1(t)$ not exceeding the limit Δ, under the control action in (13), can be denoted by

$$S_\sigma = \left\{(e_0, \tilde{e}_1) \in \mathbb{R}^2 : \left|-(k_i - k_p\alpha)e_0 - k_p\tilde{e}_1\right| \le \Delta\right\}. \tag{21}$$

By then defining

$$\bar{g}(\cdot) = \max\left\{\left|(k_i - k_p\alpha)\right|, k_p\right\} \tag{22}$$

and since $|-(k_i - k_p\alpha)e_0 - k_p\tilde{e}_1| \le \bar{g}(\cdot)(|e_0| + |\tilde{e}_1|)$, it is seen that if $\bar{g}(\cdot)(|e_0| + |\tilde{e}_1|) \le \Delta$ then $|-(k_i - k_p\alpha)e_0 - k_p\tilde{e}_1| \le \Delta$. This implies that the following set:

$$\bar{S}_\sigma = \left\{(e_0, \tilde{e}_1) \in \mathbb{R}^2 : \bar{g}(\cdot)(|e_0| + |\tilde{e}_1|) \le \Delta\right\} \tag{23}$$

by construction, must necessarily fulfill

$$\bar{S}_\sigma \subseteq S_\sigma. \tag{24}$$

Moreover, by defining

$$\bar{\bar{S}}_\sigma = \left\{(e_0, \tilde{e}_1) \in \mathbb{R}^2 : \bar{g}(\cdot)|e_0| \le \frac{\Delta}{2}, \bar{g}(\cdot)|\tilde{e}_1| \le \frac{\Delta}{2}\right\} \tag{25}$$

it immediately follows that:

$$\bar{\bar{S}}_\sigma \subseteq \bar{S}_\sigma \subseteq S_\sigma. \tag{26}$$

By keeping in mind property (26), consider the PI-controlled cantilever dynamics within (18), that is,

$$\begin{aligned}\dot{z} &= -az + b\tilde{e}_1 - b\alpha e_0 + d_1(\cdot)\\ \dot{e}_0 &= -\alpha e_0 + \tilde{e}_1\\ \dot{\tilde{e}}_1 &= \alpha_1 z + \frac{k-d^2}{d}\tilde{e}_1 - \alpha\frac{k-d^2}{d}e_0\\ &\quad - d\ C_c A_c^{-1}B_c u(t) + dC_c\tilde{x}_c - \alpha^2 e_0 + \alpha\tilde{e}_1\\ u(t) &= \bar{\alpha}\sigma(-(k_i - \alpha k_p)e_0 - k_p\tilde{e}_1) + h(\cdot)\end{aligned} \tag{27}$$

where $d_1(\cdot)$, $\tilde{x}_c$ and $h(\cdot)$ are regarded as external disturbances affecting (27). The analysis proceeds now by investigating potential invariant sets with respect to the flow in (27), with the additional property that any element within it shall not lead to system-saturation (that is, by requiring that the invariant set be contained within $\mathbb{R} \times S_\sigma$). In view of this task, by defining

$$\Omega_{\tilde{e}_1} = \left\{ \tilde{e}_1 \in \mathbb{R} : \frac{1}{2}\tilde{e}_1^2 \leq \frac{1}{2}\left(\frac{\Delta}{2\bar{g}(\cdot)}\right)^2 \right\} \tag{28}$$

it is seen that $|\tilde{e}_1| \leq (\Delta/2\bar{g}(\cdot))$ if and only if $\tilde{e}_1 \in V_{\tilde{e}_1}$. Then consider the dynamics of system (27) whenever its trajectories $(z, e_0, \tilde{e}_1)^T$ are bound to evolve solely within the set $\mathbb{R} \times S_\sigma$, that is, whenever the saturation limits are not exceeded; in such cases, it is seen that the saturation operator $\sigma(\cdot)$ behaves as the simple identity operator $\mathrm{id}(\cdot)$, that is, $\sigma(\cdot) = \mathrm{id}(\cdot)$. As a result of this, by then considering (27) along with (19) and (20), by defining

$$A = \begin{pmatrix} -a & -\alpha b \\ 0 & -\alpha \end{pmatrix}, \quad G_1 = \begin{pmatrix} b \\ 1 \end{pmatrix}, \; G_2 = \begin{pmatrix} 1 \\ 0 \end{pmatrix} \tag{29}$$

and by defining $\bar{z} = (z, e_0)^T$, simple algebraic manipulations show that the cantilever's dynamics, whenever considered to evolve within the set $\mathbb{R} \times S_\sigma$, can be given the following representation:

$$\begin{aligned} \dot{\bar{z}} &= A\bar{z} + G_1\tilde{e}_1 + G_2 d_1(\cdot) \\ \dot{\tilde{e}}_1 &= -\bar{k}_p\tilde{e}_1 - \bar{k}_i e_0 + \alpha_1 z + dC_c\tilde{x}_c + \gamma\, h(\cdot) \end{aligned} \tag{30}$$

where $\gamma = d(-C_c A_c^{-1} B_c) > 0$, $\bar{k}_p = \bar{b}k_p - (k - d^2/d) - \alpha$, $\bar{k}_i = \alpha(k - d^2/d) + \bar{b}(k_i - \alpha k_p) + \alpha^2$, $\bar{b} = d(-C_c A_c^{-1} B_c)\bar{\alpha}$, and where the quantities A, G_1 and G_2 are not dependent on the gains k_i and k_p of the control law defined in (13). Moreover, since the matrix A is Hurwitz (being $a > 0$ and $\alpha > 0$), it follows that there exists a symmetric and positive-definite matrix P such that:

$$PA + A^T P = -I. \tag{31}$$

By then defining the following quadratic form $\mathcal{V}_{\bar{z}} = \bar{z}^T P \bar{z}$, and by recalling the well-known property:

$$\lambda_{\min}(P)\|\bar{z}\|^2 \leq \bar{z}^T P \bar{z} \leq \lambda_{\max}(P)\|\bar{z}\|^2 \tag{32}$$

where $\lambda_{\min}(P)$ and $\lambda_{\max}(P)$ denote the smallest and, respectively, the largest eigenvalue of P, the following sets are defined:

$$\Omega_{\bar{z}} = \left\{ \bar{z} \in \mathbb{R}^2 : \bar{z}^T P \bar{z} \leq \lambda_{\min}(P)\left(\frac{\Delta}{2\bar{g}(\cdot)}\right)^2 \right\} \tag{33}$$

and

$$\Omega_z = \left\{ \bar{z} \in \mathbb{R}^2 : \frac{1}{2}\|\bar{z}\|^2 \leq \frac{1}{2}\left(\frac{\Delta}{2\bar{g}(\cdot)}\right)^2 \right\}. \tag{34}$$

By employing the first inequality in (32) and by multiplying both sides by $(1/2)(1/\lambda_{\min(P)})$, one obtains $(1/2)\|\bar{z}\|^2 \leq (1/2)(1/\lambda_{\min(P)})\bar{z}^T P\bar{z}$. Because of the previous inequality, it follows that if $\bar{z}^T P\bar{z} \leq \lambda_{\min}(P)((\Delta/2\bar{g}(\cdot)))^2$ then $(1/2)\|\bar{z}\| \leq (1/2)((\Delta/2\bar{g}(\cdot)))^2$, which implies that $\Omega_{\bar{z}} \subseteq \Omega_z$. In view of this, since, by construction, if $\bar{z} \in \Omega_z$ then $|e_0| \leq (\Delta/2\bar{g}(\cdot))$, it follows that if $\bar{z} \in \Omega_{\bar{z}}$ then $|e_0| \leq (\Delta/2\bar{g}(\cdot))$. By following a similar reasoning, by considering the second inequality in (32), it is seen that if $\|\bar{z}\| \leq ((\lambda_{\min}(P)/\lambda_{\max}(P)))^{1/2}(\Delta/2\bar{g}(\cdot))$ then $\bar{z} \in \Omega_{\bar{z}}$. By then defining the set

$$\Omega_{z^*} = \left\{ \bar{z} \in \mathbb{R}^2 : \frac{1}{2}\|\bar{z}\|^2 \leq \frac{1}{2}\frac{\lambda_{\min}(P)}{\lambda_{\max}(P)}\left(\frac{\Delta}{2\bar{g}(\cdot)}\right)^2 \right\} \tag{35}$$

whereby $\bar{z} \in \Omega_{z^*} \Leftrightarrow \|\bar{z}\| \leq ((\lambda_{\min}(P)/\lambda_{\max}(P)))^{1/2}(\Delta/2\bar{g}(\cdot))$, and by then using the second inequality in (32), it can be readily seen that $\Omega_{z^*} \subseteq \Omega_{\bar{z}}$. By virtue of the previous derivations, the following set-inclusions, which will be employed in the sequel, can be finally established:

$$\begin{aligned} \Omega_{z^*} \times \Omega_{\tilde{e}_1} \subseteq \Omega_{\bar{z}} \times \Omega_{\tilde{e}_1} \subseteq \Omega_z \times \Omega_{\tilde{e}_1} \subseteq \mathbb{R} \\ \times \bar{\bar{S}}_\sigma \subseteq \mathbb{R} \times \bar{S}_\sigma \subseteq \mathbb{R} \times S_\sigma. \end{aligned} \tag{36}$$

Property (36) establishes, in particular, that within the set $\Omega_{\bar{z}} \times \Omega_{\tilde{e}_1}$ the system's saturation limits are not exceeded, which implies in particular that, within such set, the dynamics of system (27) simplifies to the ones in (30).

In view of the previous derivations, it is now possible to formalize the conditions under which the system's saturation limits are not exceeded. This is done by demonstrating that there exist selections of the control gains k_p and k_i such that the previously defined set $\Omega_{\bar{z}} \times \Omega_{\tilde{e}_1}$ is invariant with respect to the flow in (30), provided that the values of the disturbances $d_1(\cdot)$, $\tilde{x}_c$ and $h(\cdot)$ be restricted to evolve within certain prescribed bounds.

To this end, in the following preliminary lemma, an algorithm for choosing the proportional and integral gains in the control law in (13) is proposed. The rationale that dictates the structure of the algorithm lies in the idea of selecting the control gains so as to render as small as desired a quantity which, in the sequel, will be shown to be strictly connected to the regulation error e_1. The lemma will be employed in the forthcoming analysis and can be regarded as describing a law by which the control gains are tuned, based on the model of the AFM system.

Lemma 1 (Gain-Tuning Algorithm): Recall that $\bar{k}_p = \bar{b}k_p - (k - d^2/d) - \alpha$, $\bar{k}_i = \bar{b}k_i - \alpha\bar{k}_p$, and that α_1 and $\bar{b}$ are positive constants, define

$$m(\alpha, \alpha_1, \bar{k}_i, \bar{k}_p) = \frac{\max\{|\bar{k}_i|,\ \alpha_1\} 4\sqrt{2}}{\bar{k}_p} \tag{37}$$

and denote $m(\alpha, \alpha_1, \bar{k}_i, \bar{k}_p)$ by $m(\cdot)$. Then, for any desired $\bar{\epsilon} > 0$, and for any $\alpha > 0$, there exists a positive number k_p^*, such that, for any $k_p \geq k_p^*$, there exists a positive gain k_i such that: the quantity $m(\cdot)$ is positive and satisfies $m(\cdot) \leq \bar{\epsilon}$.

Proof: The result follows directly by choosing the gains according to the following simple algorithm.

1) Fix α to a constant, positive value.
2) Fix k_p^* large enough such that, for any $k_p \geq k_p^*$, $\bar{k}_p$ be positive, and such that
$$\frac{\alpha_1 4\sqrt{2}}{\bar{k}_p} < \bar{\epsilon} \tag{38}$$
and fix once and for all one such k_p.
3) Finally fix k_i in $\bar{k}_i$ such that
$$|\bar{k}_i| \leq \alpha_1. \tag{39}$$

□

Define

$$\Delta_1 = \min\left\{\frac{\Delta}{2g(\cdot)}\frac{1}{6m(\cdot)\|PG_2\|} \times\sqrt{\frac{\lambda_{\min}(P)}{\lambda_{\max}(P)}}\frac{\Delta}{2g(\cdot)}\frac{1}{6\|PG_2\|}\right\}$$

$$\Delta_2 = \min\left\{\frac{\Delta}{2g(\cdot)}\frac{\bar{k}_p}{4|dC_c|},\sqrt{\frac{\lambda_{\min}(P)}{\lambda_{\max}(P)}} \times\frac{\Delta}{2g(\cdot)}\frac{\bar{k}_p}{6\|PG_1\|4|dC_c|}\right\}$$

$$\Delta_3 = \min\left\{\frac{\Delta}{2g(\cdot)}\frac{\bar{k}_p}{4\gamma},\sqrt{\frac{\lambda_{\min}(P)}{\lambda_{\max}(P)}}\frac{\Delta}{2g(\cdot)} \times\frac{\bar{k}_p}{6\|PG_1\|4\gamma}\right\} \tag{40}$$

then let $f \in \mathcal{L}^k_\infty$, and let $\|f\|_a$ denote the "asymptotic norm of f," that is $\|f\|_a = \lim_{t\to\infty}\sup\|f\|$ (see [18]). Then, in view of the previous derivations and definitions, the following theorem—which constitutes the main result of this section—can be finally demonstrated.

Theorem 2: There exist selections of the control gains k_i and k_p in (13) such that, whenever $|d_1(\cdot)| \le \Delta_1$, $\|\tilde{x}_c\| \le \Delta_2$ and $|h(\cdot)| \le \Delta_3$, then.

1) The set $\Omega_{\bar{z}} \times \Omega_{\tilde{e}_1}$ (within which the system's saturation limits are not exceeded) is invariant with respect to the flow in (30)
2) The following asymptotic bounds hold:

$$\|\tilde{e}_1\|_a \le \max\left\{6m(\cdot)\|PG_2\|\|d_1(\cdot)\|_a, \times\frac{4|dC_c|\|\tilde{x}_c\|_a}{\bar{k}_p},\frac{4\gamma\,\|h(\cdot)\|_a}{\bar{k}_p}\right\} \tag{41}$$

and

$$\|\bar{z}\|_a \le \max\left\{6\|PG_2\|\|d_1(\cdot)\|_a, 6\|PG_1\| \times\frac{4|dC_c|\|\tilde{x}_c\|_a}{\bar{k}_p}, 6\|PG_1\|\frac{4\gamma\,\|h(\cdot)\|_a}{\bar{k}_p}\right\}. \tag{42}$$

Proof: Consider the sole $\tilde{e}_1$-dynamics in (30)

$$\dot{\tilde{e}}_1 = -\bar{k}_p\tilde{e}_1 - \bar{k}_i e_0 + \alpha_1 z + dC_c\tilde{x}_c + \gamma\,h(\cdot) \tag{43}$$

and fix $k_p = k_p^{**} > 0$ large enough such that $\bar{k}_p$ be positive, while regarding e_0, z, $\tilde{x}_c$ and $h(\cdot)$ as exogenous disturbances; by then choosing $\mathcal{V}_{\tilde{e}_1} = (1/2)\tilde{e}_1^2$, the following inequality can be easily derived:

$$\dot{\mathcal{V}}_{\tilde{e}_1} \le -\bar{k}_p\tilde{e}_1^2 + \left|\bar{k}_i\right||e_0||\tilde{e}_1| + \alpha_1|z||\tilde{e}_1| + |dC_c|\|\tilde{x}_c\||\tilde{e}_1| + \gamma\,|h(\cdot)||\tilde{e}_1|. \tag{44}$$

Since $|\bar{k}_i||e_0| + \alpha_1|z| \le \max\{\alpha_1, \bar{k}_i\}(|e_0| + |z|)$ and since $|e_0| + |z| \le (2)^{1/2}\|\bar{z}\|$, then, from (44), it follows that:

$$\dot{\mathcal{V}}_{\tilde{e}_1} \le -\bar{k}_p\tilde{e}_1^2 + \max\{\alpha_1, \bar{k}_i\}\sqrt{2}\|\bar{z}\||\tilde{e}_1| + |dC_c|\|\tilde{x}_c\||\tilde{e}_1| + \gamma\,|h(\cdot)||\tilde{e}_1|. \tag{45}$$

From (45), by using the definition of the function $m(\cdot)$ in (37), the following property can be derived by employing standard arguments:

$$\dot{\mathcal{V}}_{\tilde{e}_1} \le -\frac{1}{4}\bar{k}_p\tilde{e}_1^2 \quad \text{for} |\tilde{e}_1| > \max\left\{m(\cdot)\|\bar{z}\|, \frac{4|dC_c|\|\tilde{x}_c\|}{\bar{k}_p} \times\frac{4\gamma\,|h(\cdot)|}{\bar{k}_p}\right\} \tag{46}$$

which in turn implies that

$$|\tilde{e}_1| \le \max\left\{\beta_{\tilde{e}_1}(|\tilde{e}_1(0)|, t), m(\cdot)\|\bar{z}\| \times\frac{4|dC_c|\|\tilde{x}_c\|}{\bar{k}_p},\frac{4\gamma\,|h(\cdot)|}{\bar{k}_p}\right\} \tag{47}$$

where $\beta_{\tilde{e}_1}(\cdot,\cdot)$ is a class $\mathcal{KL}$ function such that $\beta_{\tilde{e}_1}(|\tilde{e}_1(0)|, 0) = |\tilde{e}_1(0)|$. The proof proceeds now by considering the sole $\bar{z}$-dynamics within (30), that is,

$$\dot{\bar{z}} = A\bar{z} + G_1\tilde{e}_1 + G_2 d_1(\cdot) \tag{48}$$

and by regarding both $\tilde{e}_1(t)$ and $d_1(\cdot)$ as exogenous disturbances. By then considering the previously defined quadratic form $\mathcal{V}_{\bar{z}} = \bar{z}^T P\bar{z}$ as a candidate Lyapunov function, it is seen that its derivative along the trajectories of (48) satisfies

$$\dot{\mathcal{V}}_{\bar{z}} = -\|\bar{z}\|^2 + 2\bar{z}^T PG_1\tilde{e}_1 + 2\bar{z}^T PG_2 d_1(\cdot) \tag{49}$$

from which

$$\dot{\mathcal{V}}_{\bar{z}} \le -\frac{1}{3}\|\bar{z}\|^2 - \frac{1}{3}\|\bar{z}\|^2 + 2\|\bar{z}\|\|PG_1\|\|\tilde{e}_1\| - \frac{1}{3}\|\bar{z}\|^2 + 2\|\bar{z}\|\|PG_2\|\|d_1(\cdot)\| \tag{50}$$

which in turn implies that

$$\dot{\mathcal{V}}_{\bar{z}} \le -\frac{1}{3}\|\bar{z}\|^2 \quad \text{for} \|\bar{z}\| > \max\{6\|PG_1\|\|\tilde{e}_1\|, 6\|PG_2\||d_1(\cdot)|\}. \tag{51}$$

From Property (51), it is possible to infer that

$$\|\bar{z}\| \le \max\{\beta_{\bar{z}}(\|\bar{z}(0)\|, t), 6\|PG_1\|\|\tilde{e}_1\|, 6\|PG_2\||d_1(\cdot)|\} \tag{52}$$

and

$$\|\bar{z}\|_a \le \max\{6\|PG_1\|\|\tilde{e}_1\|_a, 6\|PG_2\|\|d_1(\cdot)\|_a\} \tag{53}$$

where $\beta_{\bar{z}}(\cdot,\cdot)$, in (52), is a class $\mathcal{KL}$ function such that $\beta_{\bar{z}}(|\bar{z}(0)|, 0) = |\bar{z}(0)|$; moreover, by using (52) in (47), one obtains

$$|\tilde{e}_1| \le \max\left\{\beta_{\tilde{e}_1}(|\tilde{e}_1(0)|, t), m(\cdot)\beta_{\bar{z}}(\|\bar{z}(0)\|, t) \times 6m(\cdot)\|PG_1\||\tilde{e}_1|, 6m(\cdot)\|PG_2\||d_1(\cdot)| \times\frac{4|dC_c|\|\tilde{x}_c\|}{\bar{k}_p},\frac{4\gamma\,|h(\cdot)|}{\bar{k}_p}\right\}. \tag{54}$$

The proof proceeds now by choosing the gains k_p and k_i as dictated by Lemma 1 in order to fulfill the following small-gain condition:

$$m(\cdot)\;6\|PG_1\| < 1. \tag{55}$$

By denoting by k_p^c and k_i^c the proportional and integral gains fulfilling (55), without loss of generality and in order to ease the notation, it is assumed that the already chosen proportional gain k_p^{**} satisfies $k_p^c = k_p^{**}$. Because of the small-gain inequality in (55), it is seen that $6m(\cdot)\|PG_1\||\tilde{e}_1| < |\tilde{e}_1|$. Hence, by exploiting the fact that for any positive a, b, c and $\theta(\cdot)$, if $a \leq \max\{\theta(a), b, c\}$ and $\theta(a) < a$, then $\max\{\theta(a), b, c\} = \max\{b, c\}$ (see [3, pag. 38]), it follows that property (54) can be replaced by the following inequality (which does not feature any longer the term $|\tilde{e}_1|$ on its right-hand side):

$$|\tilde{e}_1| \leq \max\left\{\beta_{\tilde{e}_1}(|\tilde{e}_1(0)|, t), m(\cdot)\beta_{\bar{z}}(\|\bar{z}(0)\|, t) \times 6m(\cdot)\|PG_2\||d_1(\cdot)|, \frac{4|dC_c|\|\tilde{x}_c\|}{\bar{k}_p} \times \frac{4\gamma\,|h(\cdot)|}{\bar{k}_p}\right\} \tag{56}$$

from which the following asymptotic bound—corresponding to inequality (41) in the theorem's statement—can be derived:

$$\|\tilde{e}_1\|_a \leq \max\left\{6m(\cdot)\|PG_2\|\|d_1(\cdot)\|_a \times \frac{4|dC_c|\|\tilde{x}_c\|_a}{\bar{k}_p}\frac{4\gamma\,\|h(\cdot)\|_a}{\bar{k}_p}\right\}. \tag{57}$$

In a similar fashion, by using (56) in (52), one obtains

$$\|\bar{z}\| \leq \max\left\{\beta_{\bar{z}}(\|\bar{z}(0)\|, t), 6\|PG_1\|\beta_{\tilde{e}_1}(|\tilde{e}_1(0)|, t) \times 6\|PG_1\|m(\cdot)\beta_{\bar{z}}(\|\bar{z}(0)\|, t), 6\|PG_1\|m(\cdot) \times 6\|PG_2\||d_1(\cdot)|, 6\|PG_2\||d_1(\cdot)|, 6\|PG_1\| \times \frac{4|dC_c|\|\tilde{x}_c\|}{\bar{k}_p}, 6\|PG_1\|\frac{4\gamma\,|h(\cdot)|}{\bar{k}_p}\right\}. \tag{58}$$

From the latter, because of the small-gain inequality in (55) which dictates that $6\|PG_1\|m(\cdot)6\|PG_2\||d_1(\cdot)| < 6\|PG_2\||d_1(\cdot)|$ and $6\|PG_1\|m(\cdot)\beta_{\bar{z}}(\|\bar{z}(0)\|, t) < \beta_{\bar{z}}(\|\bar{z}(0)\|, t)$, it is possible to derive

$$\|\bar{z}\| \leq \max\left\{\beta_{\bar{z}}(\|\bar{z}(0)\|, t), 6\|PG_1\|\beta_{\tilde{e}_1}(|\tilde{e}_1(0)|, t) \times 6\|PG_2\||d_1(\cdot)|, 6\|PG_1\|\frac{4|dC_c|\|\tilde{x}_c\|}{\bar{k}_p} \times 6\|PG_1\|\frac{4\gamma\,|h(\cdot)|}{\bar{k}_p}\right\} \tag{59}$$

and

$$\|\bar{z}\|_a \leq \max\left\{6\|PG_2\|\|d_1(\cdot)\|_a, 6\|PG_1\| \times \frac{4|dC_c|\|\tilde{x}_c\|_a}{\bar{k}_p}, 6\|PG_1\|\frac{4\gamma\,\|h(\cdot)\|_a}{\bar{k}_p}\right\}. \tag{60}$$

The asymptotic bound in (60) is indeed seen to correspond to inequality (42) in the theorem's statement. Denote now by $q_{\tilde{e}_1}(\cdot)$ the expression on the right-hand side of inequality (56) and by $q_{\bar{z}}(\cdot)$ the expression on the right-hand side of inequality (59). Then, from (56) and (59), because of the properties in (36), invariance of the set $\Omega_{\bar{z}} \times \Omega_{\tilde{e}_1}$ with respect to the flow of system (30) is guaranteed by requiring that the set $S_q = \{\bar{z} \in \mathbb{R}^2 : \|\bar{z}\| = q_{\bar{z}}(\cdot)\} \times \{\tilde{e}_1 \in \mathbb{R} : \|\tilde{e}_1\| = q_{\tilde{e}}(\cdot)\}$ be contained within $\Omega_{\bar{z}} \times \Omega_{\tilde{e}_1}$. This requirement is fulfilled by requiring that the "disturbances" $d_1(\cdot)$, $\tilde{x}_c$ and $h(\cdot)$ satisfy $|d_1(\cdot)| \leq \Delta_1$, $\|\tilde{x}_c\| \leq \Delta_2$ and $|h(\cdot)| \leq \Delta_3$ (as per the theorem's statement) and by requiring that the following two additional bounds involving the initial conditions be respected as well:

$$\beta_{\bar{z}}(\|\bar{z}(0)\|, t) \leq \frac{\Delta}{2g(\cdot)}\frac{1}{m(\cdot)}$$
$$\beta_{\tilde{e}_1}(|\tilde{e}_1(0)|, t) \leq \sqrt{\frac{\lambda_{\min}(P)}{\lambda_{\max}(P)}}\frac{\Delta}{2g(\cdot)}\frac{1}{6\|PG_1\|}. \tag{61}$$

Conditions (61) must be enforced in conformity with the fact that, as specified by the theorem's statement, the initial condition $(\bar{z}(0)\ \tilde{e}(0))^T$ must be capable of performing range within the whole set $\Omega_{\bar{z}} \times \Omega_{\tilde{e}_1}$. In view of this requirement, because $\Omega_{\bar{z}} \subseteq \Omega_z$, the first condition in (61) yields

$$\frac{\Delta}{2g(\cdot)} \leq \frac{\Delta}{2g(\cdot)}\frac{1}{m(\cdot)} \tag{62}$$

which can always be satisfied by choosing the control gains as indicated in Lemma 1 so as to render $0 < m(\cdot) \leq 1$, and by assuming that, without loss of generality, the previous choice $(k_p, k_i) = (k_p^c, k_i^c)$ fulfills such condition as well. Whereas, by definition of $\Omega_{\tilde{e}_1}$, and in view of the aforementioned requirement, the second condition in (61) yields

$$\frac{\Delta}{2g(\cdot)} \leq \sqrt{\frac{\lambda_{\min}(P)}{\lambda_{\max}(P)}}\frac{\Delta}{2g(\cdot)}\frac{1}{6\|PG_1\|} \tag{63}$$

where, after some algebra, the norm $\|PG_1\|$ in (63) is seen to satisfy

$$\|PG_1\| = \left\|\left(\frac{\alpha}{\alpha_1}\frac{k^2}{2\alpha kd + 2k^2} \quad \frac{1}{2\alpha}\right)\right\|. \tag{64}$$

From (64), and because $k = \omega_0^2$ and $d = (\omega_0/Q)$, inequality (63) is satisfied by choosing $\alpha > 0$ in the coordinate-definition in (11) sufficiently large, and then, in turn, $\alpha_1 > 0$ in the backstepping-based change of coordinate in (15) sufficiently large as well. This concludes the proof. □

IV. Piezo-Actuator Vibrational Dynamics

In this section, the stability properties of the piezo-actuator vibrational dynamics are analyzed by regarding the states $z(t), e_0(t), \tilde{e}_1(t)$ within (18) as exogenous disturbances. This is done by focusing on the relationship between ϵ and $\dot{u}$ in (18), that is, between the "speed" of the piezo-actuator vibrational dynamics and one of the controlled cantilever dynamics forced by the interaction force $F(\cdot)$ (whose time-evolution is a function of the horizontal scan rate).

In view of this task, by combining the first equation in (18) with (19), the piezo-actuator dynamics within (18) can be given the following representation:

$$\dot{\tilde{x}}_c = \frac{1}{\epsilon}A_c\tilde{x}_c + A_c^{-1}B_c\left[\bar{\alpha}\left|\frac{\partial\sigma(\bar{e})}{\partial\bar{e}}f(\cdot)\right|(a-\bar{\alpha})\sigma(\cdot) + b\frac{\partial\sigma(\bar{e})}{\partial\bar{e}}f(\cdot)\right] \tag{65}$$

where $f(\cdot)$ is defined in (20).

From the analysis in Section III, and in particular from Theorem 2, it is seen that in order not to exceed the system's saturation limits, the state variable $\tilde{x}_c$ must be bound to comply with

$$\|\tilde{x}_c\| \leq \Delta_2 \tag{66}$$

with Δ_2 defined in (40). In analogy with Section III, the task is to derive a potential invariant set with respect to flow in (65), with the additional property that any element within it satisfies the constraint in (66).

In view of this, consider the quadratic function $\mathcal{V}_{\tilde{x}_c} = \tilde{x}^T P_c \tilde{x}$, where the matrix P_c, defined as a solution of

$$P_c A_c + A_c^T P_c = -I \tag{67}$$

is guaranteed to exist symmetric and positive-definite, since A_c in (65) is Hurwitz. By then keeping in mind that

$$\lambda_{\min}(P_c) \leq \tilde{x}_c^T P_c \tilde{x}_c \leq \lambda_{\max}(P_c) \tag{68}$$

the following set is considered:

$$\Omega_{\tilde{x}_c} = \left\{\tilde{x}_c \in \mathbb{R}^m : \tilde{x}_c^T P_c \tilde{x}_c \leq \lambda_{\min}(P_c)\Delta_2^2\right\}. \tag{69}$$

By using the first inequality in (68), it is seen that if $\tilde{x}_c \in \Omega_{\tilde{x}_c}$ then the inequality in (66) must necessarily hold, implying that any element within $\Omega_{\tilde{x}_c}$ fulfills the constraint in (66), as required. It is now possible to determine under what conditions the set $\Omega_{\tilde{x}_c}$ is invariant with respect to the flow in (65) while having all of its elements fulfill the constraint in (66). This is done by considering the expression in (20), by defining $m_2(\cdot)$ as

$$\begin{aligned} m_2(\cdot) = \max\Bigg\{&\left|k_p\frac{k_d^2}{d} + k_i - \alpha k_p\right| \\ &\times \left|k_p\alpha\frac{k_d^2}{d} + k_i\alpha + \alpha^2 k_p\right|, \left|k_p\alpha_1\right| \\ &\times \left|k_p d C_c\right|, \left|k_p d C_c A_c^{-1} B_c\right|\Bigg\} \end{aligned} \tag{70}$$

then $p(\epsilon)$ as

$$p(\epsilon) = \frac{c_2 m_2(\cdot)}{\frac{1}{5}\left(\frac{1}{\epsilon} - c_2 m_2(\cdot)\right)} \tag{71}$$

where c_2 is a positive constant, and Δ_i, with $i = 4, \ldots, 7$, as

$$\begin{aligned} \Delta_4 &= \Delta_2\sqrt{\frac{\lambda_{\min}(P_c)}{\lambda_{\max}(P_c)}}\frac{1}{p(\epsilon)} \\ \Delta_5 &= \frac{1}{\sqrt{2}}\Delta_4 \\ \Delta_6 &= \Delta_4 \\ \Delta_7 &= \Delta_4 \end{aligned} \tag{72}$$

and by demonstrating the following theorem, where the stability properties of the piezo-actuator vibrational dynamics are established.

Theorem 3: Consider system (65); then, there exist $c_2 > 0$ in (71) and $\epsilon^* > 0$, such that, for any $\epsilon \leq \epsilon^*$, whenever the "disturbances" $\tilde{e}_1$, $\bar{z}$, $\sigma(\cdot)$ and $h(\cdot)$ satisfy $|\tilde{e}_1| \leq \Delta_4$, $\|\bar{z}\| \leq \Delta_5$, $|\sigma(\cdot)| \leq \Delta_6$, $|h(\cdot)| \leq \Delta_7$, then the following holds.

1) The set $\Omega_{\tilde{x}_c}$ is invariant with respect to the flow in (65).
2) The following asymptotic bound is satisfied:

$$\begin{aligned} \|\tilde{x}_c\|_a \leq \max\Bigg\{&p(\epsilon)\|\tilde{e}_1\|_a, p(\epsilon)\sqrt{2}\|\bar{z}\|_a \\ &\times p(\epsilon)\bar{\alpha}\|\sigma(\cdot)\|_a, p(\epsilon)\|h(\cdot)\|_a\Bigg\}. \end{aligned} \tag{73}$$

Proof: From (65) and (20), the derivative of $\mathcal{V} = \tilde{x}_c^T P \tilde{x}_c$ along the trajectories of system (65) reads as

$$\begin{aligned} \dot{\mathcal{V}}_{\tilde{x}_c} = &-\frac{1}{\epsilon}\|\tilde{x}_c\|^2 + 2\tilde{x}_c^T P_c A_c^{-1} B_c \\ &\times\left[\bar{\alpha}\left|\frac{\partial\sigma(\bar{e})}{\partial\bar{e}} f(\cdot)\right|(a-\bar{\alpha})\sigma(\cdot) + b\frac{\partial\sigma(\bar{e})}{\partial\bar{e}} f(\cdot)\right] \end{aligned} \tag{74}$$

from which, the following inequality can be derived:

$$\begin{aligned} \dot{\mathcal{V}}_{\tilde{x}_c} \leq &-\frac{1}{\epsilon}\|\tilde{x}_c\|^2 + 2\|\tilde{x}\|\left\|P_c A_c^{-1} B_c\right\| \\ &\times\left[\bar{\alpha}\left|\frac{\partial\sigma(\bar{e})}{\partial\bar{e}}\right||f(\cdot)||a-\bar{\alpha}||\sigma(\cdot)| \right. \\ &\left. + \left|b\frac{\partial\sigma(\bar{e})}{\partial\bar{e}}\right||f(\cdot)|\right]. \end{aligned} \tag{75}$$

Since $|(\partial\sigma(\bar{e})/\partial\bar{e})|$ is uniformly bounded, then there exists $c_2 > 0$ such that

$$\begin{aligned} 2\left\|P_c A_c^{-1} B_c\right\|&\left[\bar{\alpha}\left|\frac{\partial\sigma(\bar{e})}{\partial\bar{e}}\right||a-\bar{\alpha}||\sigma(\cdot)|\right. \\ &\left. + \left|b\frac{\partial\sigma(\bar{e})}{\partial\bar{e}}\right|\right] < c_2 \end{aligned} \tag{76}$$

hence, by using (76), the following inequality can be established from (75):

$$\dot{\mathcal{V}}_{\tilde{x}_c} \leq -\frac{1}{\epsilon}\|\tilde{x}_c\|^2 + c_2\|\tilde{x}_c\||f(\cdot)|. \tag{77}$$

Moreover, by choosing $\epsilon^* > 0$ small enough such that, for any $0 < \epsilon \leq \epsilon^*$ then $(1/\epsilon) - c_2\, m_2(\cdot) > 0$ [where $m_2(\cdot)$ has been defined in (70)], and by picking one such $\epsilon > 0$, then, from the expressions in (20)–(77), it follows that:

$$\begin{aligned} \dot{\mathcal{V}}_{\tilde{x}_c} \leq &-\left(\frac{1}{\epsilon} - c_2 m_2(\cdot)\right)\|\tilde{x}_c\|^2 + c_2 m_2(\cdot)\|\tilde{x}_c\| \\ &\times(|e_0| + |z|) + c_2 m_2(|\tilde{e}_1| + \bar{\alpha}|\sigma(\cdot)| \\ &+ |h(\cdot)|)\|\tilde{x}_c\| \end{aligned} \tag{78}$$

moreover, since $|e_0| + |z| \leq (2)^{1/2}\|\bar{z}\|$, from (78) one obtains

$$\begin{aligned} \dot{\mathcal{V}}_{\tilde{x}_c} \leq &-\left(\frac{1}{\epsilon} - c_2 m_2(\cdot)\right)\|\tilde{x}_c\|^2 + c_2 m_2(\cdot)\|\tilde{e}_1\|\|\tilde{x}_c\| \\ &+ c_2 m_2(\cdot)\sqrt{2}\|\bar{z}\|\|\tilde{x}_c\| + \bar{\alpha}|\sigma(\cdot)|c_2 m_2(\cdot)\|\tilde{x}_c\| \\ &+ |h(\cdot)|c_2 m_2(\cdot)\|\tilde{x}_c\| \end{aligned} \tag{79}$$

from which, by using standard arguments, the following property can be derived:

$$\begin{aligned} \dot{\mathcal{V}}_{\tilde{x}_c} \leq &-\frac{1}{5}\left(\frac{1}{\epsilon} - c_2 m_2(\cdot)\right)\|\tilde{x}_c\|^2 \text{for } \|\tilde{x}_c\| \\ &> \max\left\{p(\epsilon)|\tilde{e}_1|, p(\epsilon)\sqrt{2}\|\bar{z}\|\right. \\ &\left.\times p(\epsilon)\bar{\alpha}|\sigma(\cdot)|, p(\epsilon)|h(\cdot)|\right\}. \end{aligned} \tag{80}$$

Finally, from property (80), the following inequalities can be inferred:

$$\|\tilde{x}_c\| \leq \max\Big\{\beta_{\tilde{x}_c}(\|\tilde{x}_c(0)\|, t),\, p(\epsilon)|\tilde{e}_1| \times p(\epsilon)\sqrt{2}\|\bar{z}\|,\, p(\epsilon)\bar{\alpha}|\sigma(\cdot)|,\, p(\epsilon)|h(\cdot)|\Big\} \quad (81)$$

and

$$\|\tilde{x}_c\|_a \leq \max\Big\{p(\epsilon)\|\tilde{e}_1\|_a,\, p(\epsilon)\sqrt{2}\|\bar{z}\|_a \times p(\epsilon)\bar{\alpha}\|\sigma(\cdot)\|_a,\, p(\epsilon)\|h(\cdot)\|_a\Big\} \quad (82)$$

where $\beta_{\tilde{x}_c}(\cdot,\cdot)$ in (81), is a class $\mathcal{KL}$ function such that $\beta_{\tilde{x}_c}(\|\tilde{x}_c(0)\|, 0) = \|\tilde{x}_c(0)\|$. Inequality (82) corresponds to inequality (73) in the theorem's statement.

Denote by $\bar{r}(\cdot)$ the quantity on the right-hand side of (81). Then, from (81), invariance of the set $\Omega_{\tilde{x}_c}$ with respect to the flow of system (65) is guaranteed by requiring that the set $S_{\bar{r}} = \{\tilde{x}_c \in \mathbb{R}^m : \|\tilde{x}_c\| = r(\cdot)\}$ be contained within $\Omega_{\tilde{x}_c}$. By then noticing that if $\|\tilde{x}_c\|^2 \leq (\lambda_{\min}(P_c)/\lambda_{\max}(P_c))\Delta_2^2$, then $\tilde{x}_c^T P_c \tilde{x}_c \leq \lambda_{\min}(P_c)\Delta_2^2$ (that is, if $\|\tilde{x}_c\| \leq \Delta_2((\lambda_{\min}(P_c)/\lambda_{\max}(P_c)))^{1/2}$, then $\tilde{x}_c \in \Omega_{\tilde{x}_c}$), then, the aforementioned requirement is fulfilled by requiring that the "disturbances" $\tilde{e}_1$, $\bar{z}$, $\sigma(\cdot)$ and $h(\cdot)$ satisfy $|\tilde{e}_1| \leq \Delta_4$, $\|\bar{z}\| \leq \Delta_5$, $|\sigma(\cdot)| \leq \Delta_6$, $|h(\cdot)| \leq \Delta_7$ (as per the theorem's statement). This proves point 1 in the theorem's statement and concludes the proof. □

V. Closed-Loop Dynamics

By building on the results of the previous two sections, in the following, the stability properties of the closed-loop system (18) are derived as a function of the interplay between the control gains k_p and k_i, the saturation limit Δ and the "speed" ϵ of the piezo-actuator vibrational dynamics (in $\tilde{x}_c$ coordinates).

In view of this task, define

$$\begin{aligned}\bar{p}(\epsilon) &= \frac{c_2 m_2(\cdot)}{\frac{1}{4}(\frac{1}{\epsilon} - c_2 m_2(\cdot))}\\ p_1(\epsilon) &= \bar{p}(\epsilon)(1+\bar{\alpha}k_p)\\ p_2(\epsilon) &= \bar{p}(\epsilon)\Big(\sqrt{2}+\bar{\alpha}\Big)|k_i - \alpha k_p|\\ p_3(\epsilon) &= \bar{p}(\epsilon)\end{aligned} \quad (83)$$

and

$$\begin{aligned}\Delta_{d_1(\cdot)} &= \min\left\{\Delta_1,\, \Delta_2\sqrt{\frac{\lambda_{\min}(P_c)}{\lambda_{\max}(P_c)}} \times \frac{1}{\max\Big\{p_1(\epsilon)6m(\cdot)\|PG_2\|,\, p_2(\epsilon)6\|PG_2\|\Big\}}\right\}\\ \Delta_{h(\cdot)} &= \min\left\{\Delta_3,\, \Delta_2\sqrt{\frac{\lambda_{\min}(P_c)}{\lambda_{\max}(P_c)}} \times \frac{1}{\max\Big\{p_1(\epsilon)\frac{4\gamma}{\bar{k}_p},\, p_2(\epsilon)6\|PG_1\|\frac{4\gamma}{\bar{k}_p},\, p_3(\epsilon)\Big\}}\right\}\end{aligned} \quad (84)$$

where Δ_1, Δ_2, and Δ_3 have been defined in (40). Then the following result, which establishes the stability properties of the closed-loop system (18), and which constitutes the conclusive result of the last three sections, can be proven:

Theorem 4: There exist selections of the control gains k_i and k_p in (13), $\epsilon^* > 0$ small enough and $\Delta^* > 0$ large enough, such that, for any $\epsilon \leq \epsilon^*$ and $\Delta \geq \Delta^*$, whenever $|d_1(\cdot)| \leq \Delta_{d_1(\cdot)}$ and $|h(\cdot)| \leq \Delta_{h(\cdot)}$, then.

1) The set $\Omega_{\bar{z}} \times \Omega_{\tilde{e}_1} \times \Omega_{\tilde{x}_c}$ (within which, by construction, the system's saturation limits are not exceeded) is invariant with respect to the flow in (18).
2) The following asymptotic bounds hold for the states $\tilde{e}_1, \bar{z}$ and $\tilde{x}_c$:

$$\|\tilde{e}_1\|_a \leq \max\left\{6m(\cdot)\|PG_2\|\|d_1(\cdot)\|_a, \times \frac{4\gamma\,\|h(\cdot)\|_a}{\bar{k}_p}\right\} \quad (85)$$

and

$$\|\bar{z}\|_a \leq \max\left\{6\|PG_2\|\|d_1(\cdot)\|_a, 6\|PG_1\| \times \frac{4\gamma\,\|h(\cdot)\|_a}{\bar{k}_p}\right\} \quad (86)$$

and

$$\begin{aligned}\|\tilde{x}_c\|_a \leq \max\Bigg\{ &\max\Big\{p_1(\epsilon)6m(\cdot)\|PG_2\| \times p_2(\epsilon)6\|PG_2\|\Big\}\|d_1(\cdot)\|_a\\ &\times \max\Big\{p_1(\epsilon)\frac{4\gamma}{\bar{k}_p},\, p_2(\epsilon)6\|PG_1\|\frac{4\gamma}{\bar{k}_p} \times p_3(\epsilon)\Big\}\|h(\cdot)\|_a\Bigg\}.\end{aligned} \quad (87)$$

3) The following asymptotic bound holds for the original regulation error e_1:

$$\|e_1\|_a \leq \left(1+\frac{1}{\theta}\right)\max\left\{6m(\cdot)\|PG_2\|\|d_1(\cdot)\|_a \times \frac{4\gamma\,\|h(\cdot)\|_a}{\bar{k}_p}\right\} \quad (88)$$

where $\theta \in (0, 1)$.

Proof: Since within the set $\Omega_{\bar{z}} \times \Omega_{\tilde{e}_1} \times \Omega_{\tilde{x}_c}$, the operator $\sigma(\cdot)$ is such that $\sigma(\cdot) = \mathrm{id}(\cdot)$, then, within such set, the following bound can be easily established:

$$\big|\sigma(-(k_i - \alpha k_p)e_0 - k_p\tilde{e}_1)\big| \leq \big|(k_i - \alpha k_p)\big|\|\bar{z}\|\big|k_p\big|\|\tilde{e}_1|. \quad (89)$$

Pick $\epsilon_0 > 0$ small enough such that, for any $0 < \epsilon \leq \epsilon_0$ inequality (79) holds, then by using (89), from (79), the following property can be derived:

$$\begin{aligned}\dot{\mathcal{V}}_{\tilde{x}_c} \leq\ & -\Big(\frac{1}{\epsilon} - c_2 m_2(\cdot)\Big)\|\tilde{x}_c\|^2 + c_2 m_2(\cdot)\\ &\times (1+\bar{\alpha}k_p)\|\tilde{e}_1\|\|\tilde{x}_c\| + c_2 m_2(\cdot)\\ &\times (\sqrt{2}+\bar{\alpha}\big|k_i - \alpha k_p\big|)\|\bar{z}\|\|\tilde{x}_c\| + c_2 m_2(\cdot)\\ &\times |h(\cdot)|\|\tilde{x}_c\|\end{aligned} \quad (90)$$

from which, it follows that:

$$\begin{aligned}\dot{\mathcal{V}}_{\tilde{x}_c} \leq & -\frac{1}{5}\Big(\frac{1}{\epsilon}-c_2 m_2(\cdot)\Big)\|\tilde{x}_c\|^2 \text{ for } \|\tilde{x}_c\| \\ > & \max\Big\{\bar{p}(\epsilon)(1+\bar{\alpha}k_p)|\tilde{e}_1| \\ & \times \bar{p}(\epsilon)(\sqrt{2}+\bar{\alpha}\big|k_i-\alpha k_p\big|)\|\bar{z}\|,\, \bar{p}(\epsilon)|h(\cdot)|\Big\}\end{aligned} \tag{91}$$

which, in turn, leads to

$$\begin{aligned}\|\tilde{x}_c\| \leq & \max\Big\{\beta_{\tilde{x}_c}(\|\tilde{x}_c(0)\|,t),\, \bar{p}(\epsilon)(1+\bar{\alpha}k_p)|\tilde{e}_1| \\ & \times \bar{p}(\epsilon)(\sqrt{2}+\bar{\alpha}\big|k_i-\alpha k_p\big|)\|\bar{z}\|,\, \bar{p}(\epsilon)|h(\cdot)|\Big\}.\end{aligned} \tag{92}$$

Fix now the PI-control gains as $(k_p, k_i) = (k_p^c, k_i^c)$ so that the results in the statement of Theorem 2 along with the derivations within its proof, hold. By then using inequalities (56) and (59) in (92), the following expression is derived:

$$\begin{aligned}\|\tilde{x}_c\| \leq & \max\Big\{\beta_{\tilde{x}_c}(\|\tilde{x}_c(0)\|,t) \\ & \times \max\Big\{p_1(\epsilon),\, p_2(\epsilon)6\|PG_1\|\Big\}\beta_{\tilde{e}_1}(|\tilde{e}_1(0)|,t) \\ & \times \max\Big\{p_1(\epsilon)m(\cdot),\, p_2(\epsilon)\Big\}\beta_{\bar{z}}(\|\bar{z}(0)\|,t) \\ & \times \max\Big\{p_1(\epsilon)6m(\cdot)\|PG_2\|,\, p_2(\epsilon)6\|PG_2\|\Big\} \\ & \times |d_1(\cdot)|, \max\Big\{p_1(\epsilon)\frac{4\gamma}{\bar{k}_p},\, p_2(\epsilon) \\ & \qquad \times 6\|PG_1\|\frac{4\gamma}{\bar{k}_p},\, p_3(\epsilon)\Big\}|h(\cdot)| \\ & \times \max\Big\{p_1(\epsilon)\frac{4|dC_c|}{\bar{k}_p},\, p_2(\epsilon) \\ & \qquad \times 6\|PG_1\|\frac{4|dC_c|}{\bar{k}_p}\Big\}\|\tilde{x}_c\|\Big\}\end{aligned} \tag{93}$$

by then choosing $0 < \epsilon_1 \leq \epsilon_0$ small enough such that, for any $0 < \epsilon \leq \epsilon_1$ the following small-gain condition be fulfilled:

$$\max\Big\{p_1(\epsilon)\frac{4|dC_c|}{\bar{k}_p},\, p_2(\epsilon)\; 6\|PG_1\|\frac{4|dC_c|}{\bar{k}_p}\Big\} < 1 \tag{94}$$

it is seen that, for any such $0 < \epsilon \leq \epsilon_1$, the contribution of the term related to $\|\tilde{x}_c\|$ disappears from the right-hand side of inequality (93), thereby leading to the following property:

$$\begin{aligned}\|\tilde{x}_c\| \leq & \max\Big\{\beta_{\tilde{x}_c}(\|\tilde{x}_c(0)\|,t) \\ & \times \max\Big\{p_1(\epsilon),\, p_2(\epsilon)6\|PG_1\|\Big\}\beta_{\tilde{e}_1}(|\tilde{e}_1(0)|,t) \\ & \times \max\Big\{p_1(\epsilon)m(\cdot),\, p_2(\epsilon)\Big\}\beta_{\bar{z}}(\|\bar{z}(0)\|,t) \\ & \times \max\Big\{p_1(\epsilon)6m(\cdot)\|PG_2\|,\, p_2(\epsilon)6\|PG_2\|\Big\} \\ & \times |d_1(\cdot)|, \max\Big\{p_1(\epsilon)\frac{4\gamma}{\bar{k}_p},\, p_2(\epsilon) \\ & \qquad \times 6\|PG_1\|\frac{4\gamma}{\bar{k}_p},\, p_3(\epsilon)\Big\}|h(\cdot)|\Big\}\end{aligned} \tag{95}$$

from which the following asymptotic bound, which corresponds to inequality (87) in the theorem's statement, can be inferred:

$$\begin{aligned}\|\tilde{x}_c\|_a \leq & \max\Big\{\max\Big\{p_1(\epsilon)6m(\cdot)\|PG_2\|,\, p_2(\epsilon)6 \\ & \qquad \times \|PG_2\|\Big\}\|d_1(\cdot)\|_a \\ & \times \max\Big\{p_1(\epsilon)\frac{4\gamma}{\bar{k}_p},\, p_2(\epsilon)6\|PG_1\|\frac{4\gamma}{\bar{k}_p},\, p_3(\epsilon)\Big\} \\ & \times \|h(\cdot)\|_a\Big\}.\end{aligned} \tag{96}$$

In a similar fashion, by observing that any element on the right-hand side of inequality (56), with the exception of $\beta_{\tilde{x}_c}(\|\tilde{x}_c(0)\|,t))$, is multiplied by the factor $p(\epsilon)$, it follows that there exists $0 < \epsilon_2 \leq \epsilon_1$ such that, for any $0 < \epsilon \leq \epsilon_2$, by using inequality (95) in (56) and, respectively, in (59), the following bounds can be derived:

$$\begin{aligned}\|\tilde{e}_1\| \leq & \max\Big\{\beta_{\tilde{e}_1}(|\tilde{e}_1(0)|,t), m(\cdot)\beta_{\bar{z}}(\|\bar{z}(0)\|,t) \\ & \times \frac{4|dC_c|}{\bar{k}_p}\beta(\|\tilde{x}_c(0),\|,t), 6m(\cdot)\|PG_2\||d_1(\cdot)| \\ & \times \frac{4\gamma\,|h(\cdot)|}{\bar{k}_p}\Big\}\end{aligned} \tag{97}$$

and

$$\begin{aligned}\|\bar{z}\| \leq & \max\Big\{\beta_{\bar{z}}(\|\bar{z}(0)\|,t), 6\|PG_1\|\beta_{\tilde{e}_1}(|\tilde{e}_1(0)|,t) \\ & \times 6\|PG_1\|\frac{4|dC_c|}{\bar{k}_p}\beta(\|\tilde{x}_c(0),\|,t), 6\|PG_2\| \\ & \times |d_1(\cdot)|, 6\|PG_1\|\frac{4\gamma\,|h(\cdot)|}{\bar{k}_p}\Big\}.\end{aligned} \tag{98}$$

From inequality (97), the following bound on the asymptotic norm of $\tilde{e}_1$ can be inferred:

$$\|\tilde{e}_1\|_a \leq \max\Big\{6m(\cdot)\|PG_2\|\|d_1(\cdot)\|_a,\, \frac{4\gamma\,\|h(\cdot)\|_a}{\bar{k}_p}\Big\} \tag{99}$$

whereas from (98), the following bound on the asymptotic norm of $\bar{z}$ descends:

$$\begin{aligned}\|\bar{z}\|_a \leq & \max\Big\{6\|PG_2\|\|d_1(\cdot)\|_a, 6\|PG_1\| \\ & \times \frac{4\gamma\,\|h(\cdot)\|_a}{\bar{k}_p}\Big\}.\end{aligned} \tag{100}$$

Inequalities (99) and (100) correspond to inequality (85) and, respectively, inequality (86) in the theorem's statement.

Denote by $r_{\tilde{x}_c}(\cdot)$ the expression on the right-hand side of inequality (95), by $r_{\tilde{e}}(\cdot)$ the expression on the right-hand side of (97), and, finally, by $r_{\bar{z}}(\cdot)$ the expression on the right-hand side of (98). Then, from inequalities (95), (97), and (98),

invariance of the set $\Omega_{\bar{z}} \times \Omega_{\tilde{e}_1} \times \Omega_{\tilde{x}_c}$ with respect to the flow in (18) is guaranteed by requiring that the set $S_r = \{\bar{z} \in \mathbb{R}^2 : \|\bar{z}\| = q_{\bar{z}}(\cdot)\} \times \{\tilde{e} \in \mathbb{R} : \|\tilde{e}\| = q_{\tilde{e}}(\cdot)\} \times \{\tilde{x}_c \in \mathbb{R}^m : \|\tilde{x}_c\| = r_{\tilde{x}_c}(\cdot)\}$ be contained within $\Omega_{\bar{z}} \times \Omega_{\tilde{e}_1} \times \Omega_{\tilde{x}_c}$. This requirement is fulfilled by selecting $0 < \epsilon_3 \leq \epsilon_2$ and $\Delta_1 > 0$ such that, for any $0 < \epsilon \leq \epsilon_3$ and for any $\Delta \geq \Delta_1$, the "disturbances" $d_1(\cdot)$ and $h(\cdot)$ satisfy $|d_1(\cdot)| \leq \Delta_{d_1(\cdot)}$ and $|h(\cdot)| \leq \Delta_{h(\cdot)}$ (as per the theorem's statement), and by additionally requiring that the following bounds involving the initial conditions be respected as well:

$$\beta_{\tilde{e}_1}(|\tilde{e}_1(0)|, t) \leq \min\left\{\sqrt{\frac{\lambda_{\min}(P)}{\lambda_{\max}(P)}}\frac{\Delta}{2g(\cdot)} \times \frac{1}{6\|PG_1\|}, \Delta_2\sqrt{\frac{\lambda_{\min}(P_c)}{\lambda_{\max}(P_c)}} \times \frac{1}{\max\left\{p_1(\epsilon), p_2(\epsilon)6\|PG_1\|\right\}}\right\} \tag{101}$$

and

$$\beta_{\bar{z}}(\|\bar{z}(0)\|, t) \leq \min\left\{\frac{\Delta}{2g(\cdot)}\frac{1}{m(\cdot)}, \Delta_2 \times \sqrt{\frac{\lambda_{\min}(P_c)}{\lambda_{\max}(P_c)}}\frac{1}{\max\left\{p_1(\epsilon)m(\cdot), p_2(\epsilon)\right\}}\right\} \tag{102}$$

and finally

$$\beta_{\tilde{x}_c}(\|\tilde{x}_c(0)\|, t) \leq \min\left\{\frac{\Delta}{2g(\cdot)}\frac{\bar{k}_p}{4|dC_c|} \times \sqrt{\frac{\lambda_{\min}(P)}{\lambda_{\max}(P)}}\frac{\Delta}{2g(\cdot)}\frac{\bar{k}_p}{6\|PG_1\|4|dC_c|}\right\}. \tag{103}$$

Conditions (101)–(103) must be enforced in conformity with the fact that, as specified by the theorem's statement, the initial condition $(\bar{z}(0)\ \tilde{e}(0)\ \tilde{x}_c(0))^T$ must be capable to range within the whole set $\Omega_{\bar{z}} \times \Omega_{\tilde{e}_1} \times \Omega_{\tilde{x}_c}$. By keeping in mind this task, it is seen that the condition relative to the first term on the right-hand side of inequality (101) corresponds exactly to the second condition in (61), which, in Section III, has been shown to hold by choosing $\alpha > 0$ sufficiently large in (11) and then, in turn, $\alpha_1 > 0$ sufficiently large in (15). The condition corresponding to the second term on the right-hand side of inequality (101) yields

$$\frac{\Delta}{2g(\cdot)} \leq \Delta_2\sqrt{\frac{\lambda_{\min}(P_c)}{\lambda_{\max}(P_c)}} \times \frac{1}{\max\left\{p_1(\epsilon), p_2(\epsilon)6\|PG_1\|\right\}} \tag{104}$$

which is seen to hold for any $0 < \epsilon \leq \epsilon_4$, where ϵ_4 is a number satisfying $0 < \epsilon_4 \leq \epsilon_3$. The condition corresponding to the first term on the right-hand side of inequality (102) corresponds exactly to the first condition in (61), which has been shown (in the proof of Theorem 2) to hold by selecting—as it has been done—the control gains as $(k_p, k_i) = (k_p^c, k_i^c)$. On the other hand, the condition corresponding to the second term on the right-hand side of inequality (102) yields

$$\frac{\Delta}{2g(\cdot)} \leq \Delta_2\sqrt{\frac{\lambda_{\min}(P_c)}{\lambda_{\max}(P_c)}}\frac{1}{\max\left\{p_1(\epsilon)m(\cdot), p_2(\epsilon)\right\}} \tag{105}$$

which is guaranteed to hold for any $0 < \epsilon \leq \epsilon_5$, where ϵ_5 is a number satisfying $0 < \epsilon_5 \leq \epsilon_4$. Finally, by noticing that the right-hand side of (103) corresponds exactly to Δ_2, it is seen that inequality (103) is satisfied whenever $\tilde{x}_c \in \Omega_{\tilde{x}_c}$. By then fixing $\epsilon^* = \epsilon_5$ and $\Delta^* = \Delta_1$, along with $(k_p, k_i) = (k_p^c, k_i^c)$, claims 1 and 2 in the Theorem's statement are proven.

Finally, consider the third equation within system (18), that is,

$$\dot{e}_0 = -\alpha e_0 + \tilde{e}_1 \tag{106}$$

along with the Lyapunov function $\mathcal{V}_{e_0} = (1/2)e_0^2$, whose derivative along the trajectories of (106) reads as

$$\dot{\mathcal{V}}_{e_0} = -\alpha e_0^2 + \tilde{e}_1 e_0. \tag{107}$$

From (107), by picking $\theta \in (0, 1)$, it is possible to derive

$$\dot{\mathcal{V}}_{e_0} \leq -\alpha(1-\theta)e_0^2 - \alpha\theta e_0^2 + |e_0||\tilde{e}_1|$$

which leads to the following relationship between the asymptotic norms of e_0 and $\tilde{e}_1$:

$$\|e_0\|_a \leq \frac{\|\tilde{e}_1\|_a}{\alpha\theta}. \tag{108}$$

From the coordinate-definition in (15), it is seen that

$$\|e_1\|_a \leq \|\tilde{e}_1\|_a + \alpha\|e_0\|_a \tag{109}$$

which, by using (108) in (109), leads to

$$\|e_1\|_a \leq \left(1 + \frac{1}{\theta}\right)\|\tilde{e}_1\|_a. \tag{110}$$

By then combining inequalities (85) and (110), one obtains

$$\|e_1\|_a \leq \left(1 + \frac{1}{\theta}\right)\max\left\{6m(\cdot)\|PG_2\|\|d_1(\cdot)\|_a, \times \frac{4\gamma\,\|h(\cdot)\|_a}{\bar{k}_p}\right\} \tag{111}$$

where $\theta \in (0, 1)$. This proves the last claim in the theorem's statement and concludes the proof.

□

Remark 5.1: From the previous analysis, by recalling the definition in (22), it is seen that the role of the saturation Δ on the stability properties of the closed-loop system, is the one of impeding that both semiglobal and practical stability be achieved at the same time: increasing the region of attraction to any desired level, and decreasing the regulation error to any desired amount are mutually conflicting tasks. This can be seen in more detail by considering the set $\Omega_{\bar{z}} \times \Omega_{\tilde{e}_1} \times \Omega_{\tilde{x}_c}$, which, as per the results of Theorem 4, is invariant with

respect to the flow in (18), and within which, by construction, the system's saturation limits are not exceeded. Then, by using the expression in (36), which dictates that

$$\Omega_{\tilde{z}} \times \Omega_{\tilde{e}_1} \subseteq \mathbb{R} \times S_\sigma$$

and by considering the definition of S_σ in (21), it is readily seen that by increasing the control gains, the "size" of the set of states not leading to saturation may correspondingly decrease.

VI. Forming the Topography

Because the measurement mechanism employed by the AFM completely relies on its control algorithm, to the point that the actually yielded topography coincides with the control action $v(t)$, in this section, the extent to which the signal $v(t)$ is indeed capable to represent the actual topography is investigated. Such investigation is carried out by building on the stability analysis derived so far, and in the light of the detrimental phenomena represented by the system-saturation and by the actuator's vibrational dynamics and hysteresis.

The study starts by considering the dynamics in (12), and by noticing that no actuator's dynamics, nor saturation, nor control-system's dynamics is displayed within (12). Hence, if y_c were the actual commanded control signal (and, as such, also the displayed output measurement), and if the regulation error e_1 were identically equal zero, then it is easy to recognize that system (12) would embody the best possible conditions for $v(t)$ to represent $F(\cdot)$. Indeed, by recalling that $d_1(\cdot) = (1/\alpha_1)(-kx_d + (1/m)F(\cdot))$, from (12) one obtains

$$\begin{aligned} \dot{z} &= -az\frac{1}{\alpha_1}\left(-kx_d + \frac{1}{m}F(\cdot)\right) \\ y_c &= -\frac{\alpha_1}{d}z \end{aligned} \tag{112}$$

thereby showing that *in ideal conditions, the commanded control signal (which is yielded as the topography measurement) contains a filtered, and shifted version of the interaction force* $F(\cdot)$.

However, since the regulation error is not identically zero, and since y_c is not the commanded control signal, the previous analysis must be amended by including the distortion induced by the dynamics of the piezo-electric actuator implementing the control action, along with the distortion due to the presence of a nonzero regulation error. This will be done in Section VI-A.

A. Distortions Due to Nonideal Conditions

To begin with, the signal y_c within (12) is not indeed the actual commanded control signal, but is in fact generated as the output of system (4), whose input $u(t)$ is defined by (1) and (3), with $u(t) = q(t)$ in (3). By then considering system (4) along with the change of coordinates in (17) and the $\tilde{x}_c$-dynamics within system (18), an application of Tikhonov's theorem for infinite time-intervals [5, p. 439] to the solution x_c of system (4), yields

$$x_c = -A_c^{-1}B_c u(t) + \tilde{x}_c\left(\frac{t}{\epsilon}\right) + O(\epsilon) \tag{113}$$

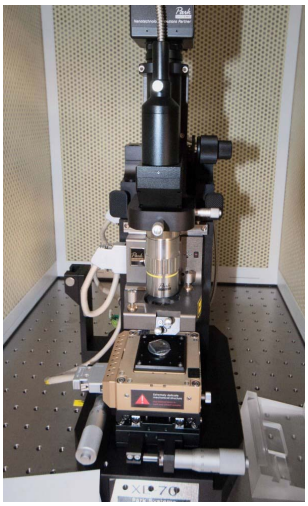

Fig. 3. AFM used for experiments.

from which, by using the output map of (4), it is possible to write

$$y_c = -C_c A_c^{-1}B_c u(t) + C_c\tilde{x}_c\left(\frac{t}{\epsilon}\right) + O(\epsilon) \tag{114}$$

which, because of (1) and (3), and by assuming that the saturation bounds are not exceeded, can be specialized as

$$y_c = -C_c A_c^{-1}B_c[\bar{\alpha}v(t) + h(\cdot)] + C_c\tilde{x}_c\left(\frac{t}{\epsilon}\right) + O(\epsilon) \tag{115}$$

that is, by solving as a function of the commanded control signal $v(t)$, as

$$v(t) = \frac{-y_c - C_c A_c^{-1}B_c h(\cdot) + C_c\tilde{x}_c\left(\frac{t}{\epsilon}\right) + O(\epsilon)}{C_c A_c^{-1}B_c\bar{\alpha}}. \tag{116}$$

Remark 6.1: Equation (116) captures in a compact fashion the distortions on the AFM imaging mechanism due to the dynamics of the piezo-electric actuator implementing the control action.

Equation (116) shows that the actual commanded control signal $v(t)$, appearing in system (12) by means of the relationship in (115), bears the contributions of both the transient $(\tilde{x}_c((t/\epsilon)))$ and steady-state $(O(\epsilon))$ of the vibrational dynamics of the piezo-actuator. While, by construction, the effect of the steady-state term $O(\epsilon)$ on $v(t)$ may be reduced by decreasing ϵ, a concurrent reduction of the effect of the magnitude of the transient term $\tilde{x}_c((t/\epsilon))$ cannot be achieved. Equation (116) highlights as well the effects of the hysteretic terms $h(\cdot)$ and $\bar{\alpha}$ on the learning mechanism, whose detrimental contribution on the yielded topography may be mitigated by resorting to hysteresis-compensation techniques such as the ones proposed in [6] and [19].

In addition, by now using (115) within the normal-form dynamics in (12), and by recalling that $d_1(\cdot) = (1/\alpha_1)(-kx_d + (1/m)F(\cdot))$, the following dynamical

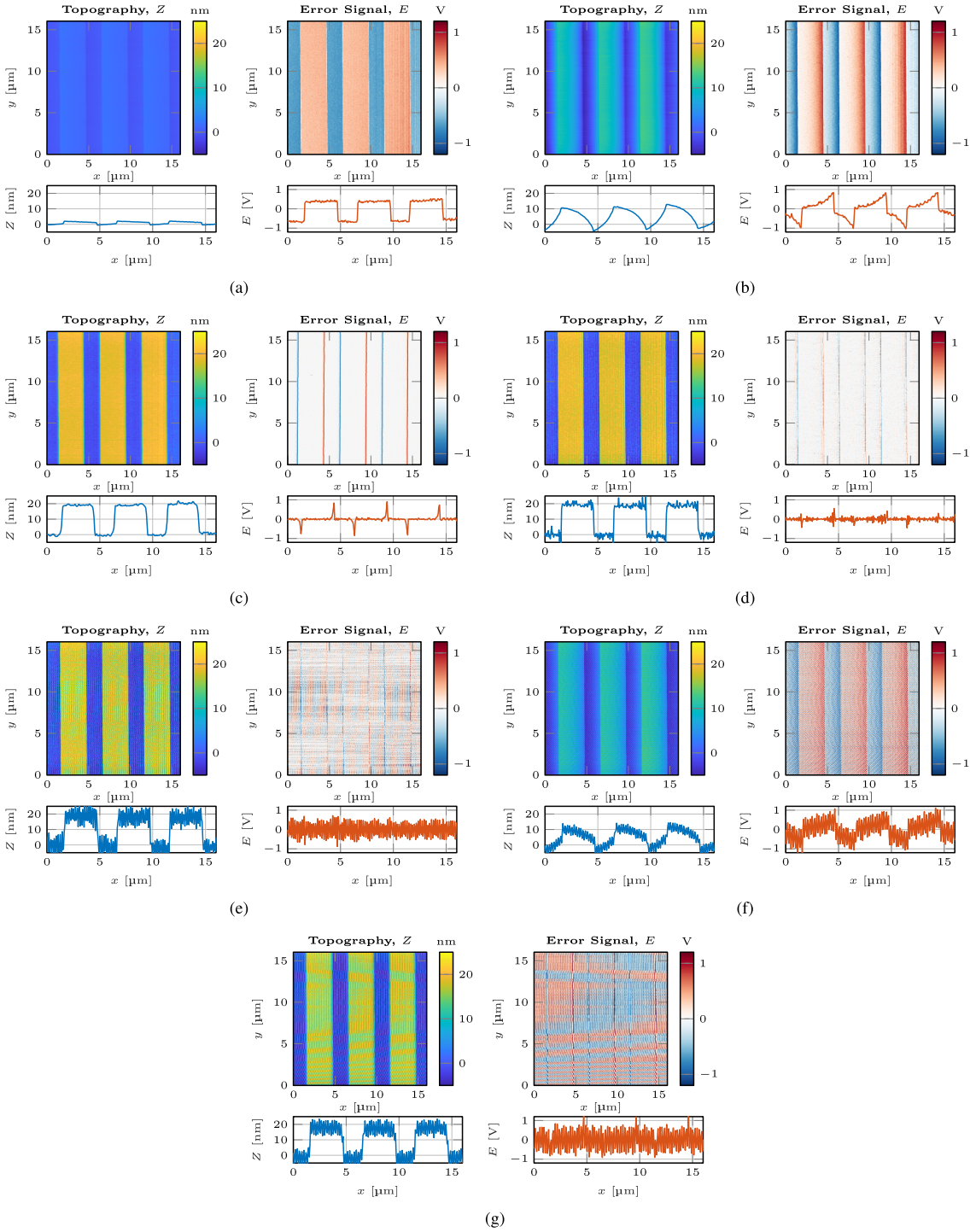

Fig. 4. AFM experiments of a calibration grating sample with step heights. The sample is scanned in contact mode using a selection of PI-parameters k_i, k_p. For each selection of parameters. the topography and the control error signal are shown, along with a cross section along the x-axis. (a) $k_i = 0.01$, $k_p = 2$. (b) $k_i = 0.2$, $k_p = 2$. (c) $k_i = 2$, $k_p = 2$. (d) $k_i = 9$, $k_p = 2$. (e) $k_i = 7.7$, $k_p = 5$. (f) $k_i = 0.2$, $k_p = 10.2$. (g) $k_i = 2$, $k_p = 9.8$.

system can be derived:

$$\begin{aligned}\dot{z} &= -az + be_1 + \frac{1}{\alpha_1}\left(-kx_d + \frac{1}{m}F(\cdot)\right)\\ \dot{e}_1 &= \alpha_1 z + \frac{k - d^2}{d}e_1 - dC_cA_c^{-1}B_c\bar{a}v(t)\\ &\quad - d\ C_cA_c^{-1}B_ch(\cdot) + dC_c\tilde{x}_c\left(\frac{t}{\epsilon}\right) + O(\epsilon). \qquad (117)\end{aligned}$$

Because of the presence of e_1 within (117), it is seen that a further source of distortion on the AFM-imaging mechanism is due to the inherent impossibility of keeping the regulation error e_1 to zero. Such detrimental effect can immediately be observed from the z-dynamics within system (117), which shows that the information about the interaction force $F(\cdot)$ contained within the output variable z, is altered by the presence of a nonzero e_1. As per the stability analysis presented

in Sections III–V, the reduction of the regulation error e_1 is not only affected by the detrimental effects due to the piezo-actuator, but by the system-saturation as well, which impedes that both semiglobal and practical stability be achieved at the same time.

It is also worth stressing the following:

Remark 6.2: The dynamics of the PI control law in (13) has not produced any explicit contribution toward the derivation of the expression in (117). This implies that the validity of (117) extends beyond the use of a proportional-integral algorithm. Indeed, (117) describes the inherent AFM-imaging mechanism of any possible control algorithm employed in contact mode, whenever the boundaries imposed by the saturation limits are respected.

VII. Experimental Results

In this section, which complements the theoretical contributions exposed so far, a set of AFM imaging experiments is reported, with the aim of relating the observed experimental evidences to the derived theoretical results.

The proposed experiments were performed in contact mode on a commercial AFM (Park Systems XE-70) displayed in Fig. 3, which was set up to be representative of a typical contact mode imaging experiment, and whose control loop is reflected by the diagram shown in Fig. 1. The AFM is controlled using a Windows desktop machine running the Park Systems XEP software. The desktop machine is connected to an external Park Systems SPM controller where the control algorithm is implemented, and all input–output signals are measured and generated. The sample positioning is controlled by separate piezoelectric XY- and Z-scanners, thereby enabling independent axis control. The XY-scanner is a body-guided flexure scanner with a range of 50 μm $\times$ 50 μm; the Z-scanner, mounted on the head of the AFM (above the sample), features a movement range of 12 μm. The deflection measurement is generated by a PSPD. The image resolution was set to 256 $\times$ 256.

The integrated PI control law was used and set up such that the PI gains could be specified independently. The sample used (BudgetSensors HS-20MG) is a calibration grating with periodic features of 20 nm step height. The scans were performed over the sample's step lines in the y-direction featuring a 5 μm pitch, at a scan-size of 16 μm $\times$ 16 μm area of the sample. Thus, the performance of the control law could be observed as the steps of the sample were scanned by the cantilever. The scanning rate was set to 5 Hz for all imaging experiments. The parameters of the PI control law were changed between experiments, resulting in topography and error measurements for a collection of PI parameters, as shown in Fig. 4.

From the experimental results reported from Fig. 4(a) to Fig. 4(c), it is possible to observe a trend of steady improvement of the imaging-quality as the integral gain is increased from $k_i = 0.01$ to $k_i = 2$, while the proportional gain is kept constant at $k_p = 2$. This behavior appears compatible with the results of Theorem 4 (along with Remark 5.1): indeed, because of inequality (88), by definition of $m(\cdot)$ and $\bar{k}_p$, Theorem 4 stipulates that by choosing the proportional gain k_p sufficiently large, it is always possible to choose the integral gain k_i so as to steer the regulation e_1 toward an attractor whose size can be made as small as desired, provided the boundaries imposed by the saturation mechanism be respected.

The inception of image-degradation is then observed when at least one of the two control gains is large [from Fig. 4(d) to Fig. 4(g)]: this is compatible with the presence of the saturation mechanism, whose detrimental effect manifests itself in the shrinking of the "size" of the set of initial conditions not leading to saturation as the values of the control gains are increased, as stressed within Remark 5.1.

By now considering the first equation within (18) along with the change of variable in (17), because the experiments have not been carried out at a high scan-rate, it can be expected that the vibrational dynamics x_c of the piezo-actuator are such to evolve at a much faster rate than the ones of the controlled cantilever dynamics. This is because the time-evolution of the x_c-dynamics directly depends on the interaction force $F(\cdot)$, which is in turn, a function of the horizontal scan rate. That is, it can be expected that the steady-state of the vibrational dynamics of the piezo-actuator [represented by the term $O(\epsilon)$ in (116)] is such to contribute toward the observed image-degradation only to a minor extent. Such behavior is furthermore reflected by having ϵ small enough in the first equation in (18) so as to be capable of performing off-set the effect of $\dot{u}$ on the evolution of $\tilde{x}_c$, or, equivalently, so as the make the right-hand side of inequality (95) negligible. On the other hand, by virtue of the analysis pursued in Section VI-A, both the transient value $\tilde{x}_c((t/\epsilon))$ of the piezo-actuator vibrational-dynamics and the terms representing the hysteresis perturbation in (116), are expected to provide a nonnegligible contribution to the experimentally observed topography-distortions.

VIII. Conclusion

This work has proposed an investigation of the properties, from a nonlinear control standpoint, of AFMs operated in contact mode and controlled by a PI control law. By regarding the AFM-system as an architecture within which a piezo-electric actuator and a cantilever mutually interact in order to produce the sample-topography, image-degrading phenomena due to hysteresis and vibrational-dynamics within the piezo-actuator, or caused by system-saturation, have been naturally cast and analyzed. In spite of the inherently nonlinear nature of the AFM dynamics, investigations of the contact mode case from a nonlinear standpoint had been lacking within the AFM literature. This article has filled this gap, by providing a study in which the very meaning of the image-measurement yielded by the AFM—whenever operated in contact mode with a PI algorithm—is investigated, in the light of distortions due to the nonlinear nature of the AFM. Furthermore, as a byproduct of the derived nonlinear stability analysis, a novel, model-based algorithm for tuning the PI control gains has been provided. Finally, experimental results have been presented and analyzed in the light of the derived theory.

References

[1] P. Eaton and P. West, *Atomic Force Microscopy*. London, U.K.: Oxford Univ. Press, 2010.

[2] N. Jalili and K. Laxminarayana, "A review of atomic force microscopy imaging systems: Application to molecular metrology and biological sciences," *Mechatronics*, vol. 14, no. 8, pp. 907–945, Oct. 2004.
[3] A. Isidori, *Nonlinear Control System II*. London, U.K.: Springer-Verlag, 2000.
[4] A. Isidori, *Nonlinear Control System*. London, U.K.: Springer-Verlag, 1995.
[5] H. Khalil, *Nonlinear System*. Hoboken, NJ, USA: Prentice-Hall, 2002.
[6] A. Esbrook, X. Tan, and H. K. Khalil, "Inversion-free stabilization and regulation of systems with hysteresis via integral action," *Automatica*, vol. 50, no. 4, pp. 1017–1025, 2014.
[7] A. Visintin, *The Science of Hysteresis*. London, U.K.: Academic, 2006.
[8] J. Yi, S. Chang, and Y. Shen, "Disturbance-observer-based hysteresis compensation for piezoelectric actuators," *IEEE/ASME Trans. Mechatronics*, vol. 14, no. 4, pp. 456–464, Aug. 2009.
[9] C.-Y. Su, Y. Stepanenko, J. Svoboda, and T. P. Leung, "Robust adaptive control of a class of nonlinear systems with unknown backlash-like hysteresis," *IEEE Trans. Autom. Control*, vol. 45, no. 12, pp. 2427–2432, Dec. 2000.
[10] M. Edardar, X. Tan, and H. K. Khalil, "Tracking error analysis for feedback systems with hysteresis inversion and fast linear dynamics," *J. Dyn. Syst., Meas., Control*, vol. 136, no. 4, Jul. 2014, Art. no. 041010, doi: 10.1115/1.4026511.
[11] Y. Fang, M. Feemster, D. Dawson, and N. M. Jalili, "Nonlinear control techniques for an atomic force microscope system," *J. Control Theory Appl.*, vol. 3, no. 1, pp. 85–92, Feb. 2005.
[12] R. García and A. S. Paulo, "Dynamics of a vibrating tip near or in intermittent contact with a surface," *Phys. Rev. B, Condens. Matter*, vol. 61, no. 20, pp. R13381–R13384, May 2000.
[13] S. I. Lee, S. W. Howell, A. Raman, and R. Reifenberger, "Nonlinear dynamics of microcantilevers in tapping mode atomic force microscopy: A comparison between theory and experiment," *Phys. Rev. B, Condens. Matter*, vol. 66, Sep. 2002, Art. no. 115409.
[14] G. Schitter, P. Menold, H. F. Knapp, F. Allgöwer, and A. Stemmer, "High performance feedback for fast scanning atomic force microscopes," *Rev. Sci. Instrum.*, vol. 72, no. 8, pp. 3320–3327, 2001.
[15] D. Platz, D. Forchheimer, E. A. Tholén, and D. B. Haviland, "Interaction imaging with amplitude-dependence force spectroscopy," *Nature Commun.*, vol. 4, no. 1, pp. 1–9, Jun. 2013.
[16] Y. Fang, M. Feemster, D. Dawson, and N. Jalili, "Active interaction force identification for atomic force microscope applications," in *Proc. 41st IEEE Conf. Decis. Control*, vol. 4, Dec. 2002, pp. 3678–3683.
[17] M. Krstic, P. V. Kokotovic, and I. Kanellakopoulos, *Nonlinear and Adaptive Control Design*, 1st ed. New York, NY, USA: Wiley, 1995.
[18] A. R. Teel, "A nonlinear small gain theorem for the analysis of control systems with saturation," *IEEE Trans. Autom. Control*, vol. 41, no. 9, pp. 1256–1270, Sep. 1996.
[19] A. Esbrook, X. Tan, and H. K. Khalil, "Control of systems with hysteresis via servocompensation and its application to nanopositioning," *IEEE Trans. Control Syst. Technol.*, vol. 21, no. 3, pp. 725–738, May 2013.

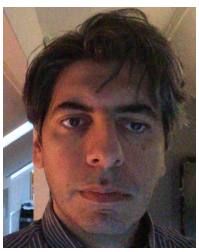

Saverio Messineo received the Ph.D. degree in control systems from the Norwegian University of Science and Technology (NTNU), Trondheim, Norway, in 2009.

During his research career, he has been engaged in the investigation of problems within the area of control systems, either within an industrial framework (e.g., as a Research Scientist with the Schlumberger Gould Research Centre, Cambridge, U.K.), or in academia, while holding the post of an Associate Professor in control systems with NTNU. From a theoretical standpoint, his research interests lie in the field of adaptive and robust nonlinear control design, nonlinear observer design, quasi-periodic disturbance rejection, and nonlinear output regulation. In relation to the applicative side, he has been working in the experimental investigation of areas such as offshore crane control for marine operations, control of directional drilling systems for petroleum engineering applications, control of atomic force microscopes, and active vibration rejection for metrology platforms within the context of precision control for mechatronics systems.

Michael R. P. Ragazzon (Member, IEEE) received the M.Sc. and Ph.D. degrees in engineering cybernetics from the Norwegian University of Science and Technology (NTNU), Trondheim, Norway, in 2013 and 2018, respectively.

He is currently a Post-Doctoral Researcher in atomic force microscopy with NTNU. His main research interests include control theory and parameter estimation, and their application to extending the imaging capabilities of atomic force microscopes.

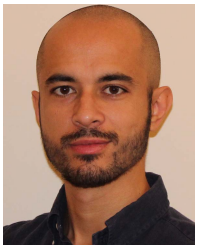

Fabio Busnelli received the Ph.D. degree in systems and control from the Politecnico di Milano, Milan, Italy, in 2017.

He has been a Researcher with the Institute of Automation and Control, TU Wien, Vienna, Austria, Vienna, followed by his Ph.D. research in vehicle dynamics. His current research focuses include modeling and control for hybrid and electrical vehicles. His research interests include optimal control and dynamics control with emphasis on their application in mechatronics systems and automotive applications.

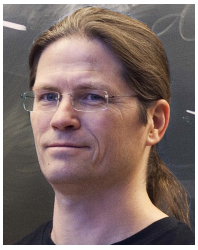

Jan Tommy Gravdahl (Senior Member, IEEE) received the Siv.ing. and Dr.ing. degrees in engineering cybernetics from the Norwegian University of Science and Technology (NTNU), Trondheim, Norway, in 1994 and 1998, respectively.

Since 2005, he has been a Professor with the Department of Engineering Cybernetics, NTNU, where he also served as the Head of Department, from 2008 to 2009. He has supervised the graduation of 150 M.Sc. and 14 Ph.D. candidates. He has published five books and more than 250 articles in international conferences and journals. His current research interests include mathematical modeling and nonlinear control in general, in particular applied to turbomachinery, marine vehicles, spacecraft, robots, and high-precision mechatronic systems.

Mr. Gravdahl was a recipient of the IEEE TRANSACTIONS ON CONTROL SYSTEMS TECHNOLOGY Outstanding Paper in 2000 and 2017. Since 2017, he has been a Senior Editor of the *IFAC Journal Mechatronics*, where he also served as an Associate Editor since 2016, and since 2020, he has been an Associate Editor of the IEEE TRANSACTIONS ON CONTROL SYSTEMS TECHNOLOGY. He has been on the editorial board and IPC for numerous international conferences.